METAL OXIDE NANOPARTICLE COATINGS FOR ENHANCED MECHANICAL AND CHEMICAL PROPERTIES OF GLASS FIBERS

A THESIS SUBMITTED TO

THE GRADUATE SCHOOL OF ENGINEERING AND SCIENCE

OF BILKENT UNIVERSITY

IN PARTIAL FULFILLMENT OF THE REQUIREMENTS FOR

THE DEGREE OF

MASTER OF SCIENCE

IN

MATERIALS SCIENCE AND NANOTECHNOLOGY

By

Arda Kurucu

January 2024

Metal oxide nanoparticle coatings for enhanced mechanical and chemical properties of glass fibers
By Arda Kurucu
January 2024

We certify that we have read this thesis and that in our opinion it is fully adequate, in scope and in quality, as a thesis for the degree of Master of Science.

Bülend Ortaç(Advisor)

Mustafa Ordu(Co-Advisor)

Mehmet Yılmaz

Yusuf Keleştemur

Approved for the Graduate School of Engineering and Science:

Orhan Arıkan
Director of the Graduate School

ABSTRACT

METAL OXIDE NANOPARTICLE COATINGS FOR ENHANCED MECHANICAL AND CHEMICAL PROPERTIES OF GLASS FIBERS

Arda Kurucu
M.S. in Materials Science and Nanotechnology
Advisor: Bülend Ortaç
Co-Advisor: Mustafa Ordu
January 2024

Glass fibers are one of the most used reinforcement fibers in composites. They have highly demanded properties such as good mechanical properties, impact resistance, high strength-to-weight ratio, and cost-efficiency. Glass fiber composites are utilized in many fields such as aerospace, automotive, and maritime. Glass fibers are one of the components in the composite structure aside from the resin matrix and their properties heavily affect the overall properties of the composite material. By improving the properties of glass fiber reinforcement, composite performance can also be improved. Industrial-scale fabrication of glass fiber requires the construction of a certain glass-type exclusive factory. This study aims to have an alternative solution to meet the strength demands of industry with a relatively simple modification to the production process of E-glass fibers. In this study, the mechanical, chemical, and dielectric properties of glass fibers are altered via metal oxide nanoparticle coating. A thin layer of ZnO coating is applied onto the E-glass fibers via the dip coating method. Through spectroscopic and SEM characterization, the presence of ZnO coating is confirmed, and the effect of this coating on mechanical properties is investigated through micromechanical analysis. ZnO coating proved to increase the tensile strength of E-glass fibers by 14.67%. In addition to mechanical improvements, the ZnO nanoparticles proved to be effective in corrosion resistance. Their corrosion-resistant properties are investigated using an acidic environment. Coated fibers are then used to manufacture a glass fiber felt composite to investigate the effect of nanoparticles on signal transmittance properties of glass fiber composites. In addition to the modification of common E-glass fibers, a novel pure silica fiber fabrication method for advanced aerospace composite applications is developed. Principles of optical fiber production are utilized to fabricate structural high-purity fiber with unconventional fuel gas heating sources. This study aims to obtain know-how and knowledge on the production of pure silica fiber. To fabricate the pure silica fiber, a novel custom fabrication setup is designed and manufactured. This setup includes a custom heating system, a custom capstan tractor, and a custom feeding system.

Keywords: Glass fibers, Mechanical properties, Chemical properties, Acid resistance, Composites, Fiber fabrication method, Fiber fabrication equipment.

ÖZET

CAM ELYAFLARN GELIşMIş MEKANIK VE KIMYASAL ÖZELLIKLERI IÇIN METAL OKSIT NANOPARTIKÜL KAPLAMALAR

Arda Kurucu
Malzeme Bilimi ve Nanoteknoloji, Yüksek Lisans
Tez Danışmanı: Bülend Ortaç
İkinci Tez Danışmanı: Mustafa Ordu
Ocak 2024

Cam elyaflar kompozitlerde en çok kullanılan takviye elyaflarından biridir. iyi mekanik özellikler, darbe direnci, yüksek mukavemet/ağırlık oranı ve maliyet verimliliği gibi oldukça talep gören özelliklere sahiptirler. Cam elyaf kompozitler havacılık, otomotiv ve denizcilik gibi birçok alanda kullanılmaktadır. Cam elyaflar kompozit yapıdaki reçine matrisinin yanı sıra bileşenlerden biridir ve özellikleri kompozit malzemenin genel özelliklerini büyük ölçüde etkilemektedir. Cam elyaf takviyesinin özelliklerinin iyileştirilmesiyle kompozit performansı da geliştirilebilir. Cam elyafın endüstriyel ölçekte üretimi, belirli bir cam tipi özel fabrikanın inşasını gerektirir. Bu çalışma, E-cam elyafların üretim prosesinde nispeten basit bir modifikasyon ile endüstrinin mukavemet taleplerini karşılamak için alternatif bir çözüm bulmayı amaçlamaktadır. Bu çalışmada, cam elyafların mekanik, kimyasal ve dielektrik özellikleri metal oksit nanoparçacık katkılaması yoluyla değiştirilmektedir. Daldırma kaplama yöntemiyle E-cam elyafların üzerine ince bir ZnO kaplama tabakası uygulanır. Spektroskopik ve SEM karakterizasyonuyla ZnO kaplamanın varlığı doğrulanır ve bu kaplamanın mekanik özelliklere etkisi mikromekanik analizle araştırılır. ZnO kaplamanın E-cam elyafların çekme mukavemetini %14,67 oranında arttırdığı ve kırılma olasılığını azalttığı gözlemlenmiştir. Mekanik iyileştirmelerin yanı sıra ZnO nanopartiküllerinin korozyon direncinde de etkili olduğu gözlemlenmiştir. Korozyona dayanıklı özellikleri asidik bir ortam kullanılarak araştırılır. Kaplanmış fiberler daha sonra nanopartiküllerin cam fiber kompozitlerin sinyal iletim özellikleri üzerindeki etkisini araştırmak için bir cam fiber keçe kompozit üretmek için kullanılır. Yaygın E-cam elyafların modifikasyonuna ek olarak, ileri havacılık kompozit uygulaması için yeni bir saf silika elyaf üretim yöntemi geliştirildi. Optik fiber üretiminin ilkeleri, geleneksel olmayan yakıt gazı ısıtma kaynağıyla yapısal yüksek saflıkta fiber üretmek için kullanılır. Bu çalışma, saf silika elyaf üretimine ilişkin teknik bilgi elde etmeyi amaçlamaktadır. Saf silika elyafını üretmek için yeni bir özel imalat düzeneği tasarlandı ve üretildi. Bu kurulum, özel bir ısıtma sistemi, özel ırgat traktörü ve özel bir besleme sistemi içerir.

Anahtar sözcükler: Cam elyaf, Mekanik özellikler, Kimyasal özellikler, Asit direnci, Kompozitler, Fiber üretim metodu, Fiber üretim ekipmanı.

Acknowledgement

I would like to start by thanking my advisor, Dr. Mustafa Ordu, for giving me this opportunity to work and study in his research group, Contemporary Fibers Laboratory. His guidance and support allowed me to complete my master's degree. Additionally, I would like to thank all the past and present members of CFL, including the past members Ali Bagheri Behboud and Md. Kawsar Ahmed pioneered the structural fiber branch in our research group. I especially thank our undergraduate interns, Göktan Yılmaz and Sude Pelin Öçalan, for their assistance in the completion of the experiments. I would also like to thank our industrial partners, SISECAM Inc. and Turkish Aerospace Industries, for their support. Also, special thanks to our group engineer and my friend Cihat Kürşat Kalkan for making the silica fabrication experience as much fun as possible. I would like to thank all my friends at UNAM for creating a friendly and comfortable environment through my master's degree.

I would like to thank the UNAM facility and engineers in UNAM, Hansa Dolaş, Zeynep Tunalı, Burcu Durmuş, Sevcan Berivan Uğur, Esra Arman Karaaslan, Abdulsamet Özcan, and Can Güven for being understanding and continuous assistance.

Above all, thank you to my mother, Gulcin, and father, Bayar, for supporting me through all my decisions and encouraging me to pursue this master's degree. They ensured I had access to the best education they could provide.

And finally, the love of my life, Alara, helped me get through the toughest times with kindness and encouragement. Her support through my bachelor's degree allowed me to always aim for the better.

Contents

List of Figures

List of Tables

Chapter 1

Introduction

Glass fibers have been used as reinforcement materials in composites owing to their excellent mechanical and chemical properties, providing a high strength-to-weight ratio, production scalability, and cost-efficiency compared to alternative reinforcement materials[3, 4, 5, 6].

Glass fibers were used as excellent electrical insulators. Besides their electrical insulation properties, glass fibers act as excellent thermal insulators and are used in various fields, including construction, pipelines, and transportation [6]. The strength-to-weight ratio of a structural glass fiber composite outperforms many other materials in fields in which weight reduction is desired, such as aerospace and aviation.

The combination of reinforcement and matrix results in the utilization of both the desired properties of two materials [3]. Ultimately, the overall quality of the composite end product is driven by the quality of both glass fibers and the epoxy resin.

In this thesis, the utilization of glass fibers as reinforcement material for aerospace composite applications is comprehensively discussed. The structure of the work is the following: in the first section, a historical overview of glass fibers is covered. The following sections provide insight into the manufacturing processes, types, and properties of glass fibers. Subsequently, applications of glass fibers in various fields are detailed. Finally, the future prospects of glass fibers, including opportunities and challenges, are critically discussed at the end of the work.

1.1 Historical Overview of Glass Fibers

Glass has been manufactured in various shapes and forms. One very versatile form that has been widely used in many different applications is glass fiber. First-ever glass fiber was fabricated through the ancient Eygpt in approximately 100 BC. This was before the invention of the glass-blowing technology. After this, in the relatively closer past, there were appearances of glass fibers on Venetian dishes manufactured in the 16th century. Being relatively primitive, they were not continuous and appeared as small bundles of glass fiber [3].

Demand for glass fiber deviated from the decoration of dishes to the textile industry in the early 1700s. French scientist René Antoine Ferchault de Réaumur decorated textiles with the glass fibers that he produced in 1713. Different from previous methods to fabricate glass fibers, he used molten glass instead of forming glass rods heated past their glass transition temperature. This also is considered to be the invention of glass fiber [3, 7]. Production of glass fiber from molten glass material opened a door for the trials of continuous glass fiber fabrication. Many inventors tried to scale up the continuous fabrication of glass fibers throughout the 1800s. In 1822, British inventors carried out an experiment of this kind. A glass dress made using British silk looms was displayed at the 1893 Columbian Exposition in Chicago, while another inventor, Edward Liebey, also used glass at the 1842 British silk loom [3]. The first succesful continuous glass fiber fabrication was recorded in 1893 by Edward Drummond Libbey, who displayed clothing composed of glass fiber and silk [5]. After the successful demonstration of a long-length glass fiber, the first application of the glass fiber was performed in a fabric with silk and glass mix [6]. In 1938, the first patent for glass fiber was issued for manufactured glass fiber wool by Russel Games Slayter [8]. The manufactured glass fibers are marketed under the commercial name of "Fiberglas". As the glass wool performs as an excellent electrical insulator, the produced glass fibers are classified as E-glass fibers, getting the letter "E" for electrical as the mentioned application. Besides the electrical insulation properties, glass fibers act as an excellent thermal insulator and are used as such in various fields. These types of insulators were used in World War 2 era US Navy warships [6]. The strength-to-weight ratio of a structural glass fiber composite outperforms many other materials in fields in which weight reduction is desired, such as aerospace and aviation.

Structural glass fibers come in glass fiber composite form for aerospace and aviation applications. Fibers are generally combined with an epoxy/resin matrix to act as reinforcement components. The combination of reinforcement and matrix results in the utilization of both the desired properties of two materials [9]. Ultimately, the overall quality of the composite end product is driven by the quality of both glass fibers and the epoxy resin. After the introduction of glass fibers in the US Navy in 1939, glass fibers were further used as a reinforcement component for glass fiber composites in warplanes during the World War 2 era. Mainly utilizing the strength-to-weight ratio and signal transmittance properties, the glass fiber composites were used to produce radomes and other structural components using the straightforward hand layup method [6].

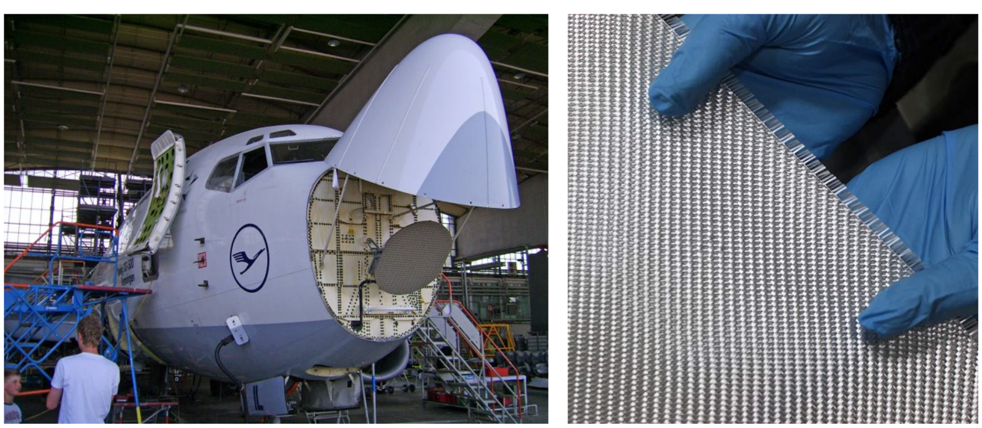

Figure 1.1: Images of a radome on a commercial airplane and glass fiber fabric [1, 2].

After World War 2, glass fiber composites were introduced to the regular consumer market as structural components for the automobile industry. Utilizing the high strength-to-weight ratio, they were used to reduce the weight of the vehicle without compromising the strength requirements. Reduction of weight results in high fuel efficiency and high speed demanding performance. Today, the usage of glass fiber-reinforced composites covers wide application fields, including renewable energy, transportation (automobile, ship and aerospace), construction, and defense. The aerospace industry still utilizes glass fiber composites on numerous parts of airplanes, including the main body, wing ends, and tails.

The modern market for composite materials is heavily dominated by glass fiber composites, which they are supplying 95% of the global raw material demand for reinforcement components, making them the most popular material for such applications. There are different types of glass fibers in the market. However, the market is currently heavily dominated by E-type glass fibers [10, 11].

1.2 Manufacturing Process of Glass Fibers

The modern glass manufacturing industry is oriented around direct plant manufacturing processes that require a designated production plant dedicated solely to producing glass fiber for a high product yield. The production of the glass fiber starts with the silos containing raw material on top of a mixing tank. Weighing and combining specific raw materials is the first step in the melting process of glass. This procedure is highly automated in contemporary fiberglass facilities, complete with enclosed material transport systems and electronic weighing machines. Before being sent to the furnace, the separate parts are weighed and brought to a blending station where the batch materials are completely blended [3]. These materials are a mix of different percentages of silica clay that has alumina, boric acid, or colemanite, which has boron oxide, and limestone, which has calcium oxide. These raw materials are generally used in the manufacturing of E-glass fibers. As the materials are being mixed, they are transported into the furnace section to be fully melted. The whole system is separated from the atmosphere with an air-tight setup to prevent impurities such as dust from contaminating the production line[6].

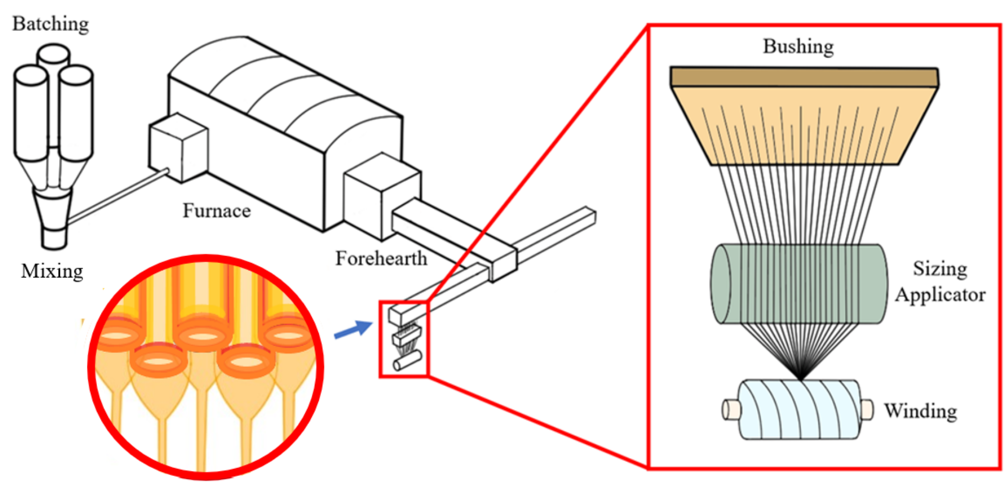

Figure 1.2: Schematic diagram of continuous glass fiber fabrication and close view of bushing.

Glass fiber furnaces usually have a narrow and short forehearth channel that carries molten glass material to the bushing section.

In order to preserve the heat and increase efficiency, the furnace walls are constructed from one of the best refractory materials. The refractories have decisive impacts on furnace design that controls the product (glass fiber) quality, product cost, and energy consumption and have complicated structures/combinations to achieve these. The refractory materials are generally ceramics and could be made out of alumina, zirconia, magnesia, dense chromium oxide, silica clay, or a mixture of these materials. The material selection also depends on the section of the furnace that faces different temperatures and materials, as well as the composition of glass fibers. which is preferred for its corrosion resistance property against the molten E-glass material [6]. The refractory layer is covered by zircon blocks, and then another layer of clay blocks is added to increase the thermal insulation further. Currently, the fabrication of industrial-scale glass fibers is heavily dependent on natural gas. The inside of the furnace reaches between 1400 and 1700°C, past the melting point of raw materials. The operating temperature of the furnace is dependent on the type of glass fiber that is manufactured. There are electrodes and bubblers located in the bottom section of the furnace. They interact with the molten glass, removing the gases and finalizing the chemical reactions [6]. Coming out of the furnace, molten material reaches the forehearth part of the production line, as seen in Figure 1.2. The forehearth temperature is slightly lower than the temperature of the furnace part. Finally, through the forehearth section, cooled molten glass material reaches the bushing section. The bushing is constructed from a special alloy that contains platinum and rhodium in its composition. This is done so that the bushing can withstand high-temperature conditions and the corrosive effect of the molten glass material. Rhodium is preferred for its high stiffness and high hardness properties. Platinum is preferred for its excellent corrosion resistance against molten glass. The bushing is also used for further temperature control for the production via electrical heating and monitoring. This also helps keep the temperature uniform at the end of the thermal production line. The nozzle diameter for the bushing is between 0.75 to 2.0 mm, and the winder pulls the fiber down with speeds up to 60 m/s [12]. The production speed depends on various parameters, such as the size of openings on the bushing, length of the opening, and glass viscosity. Bushing contains small holes and nozzles that the molten glass material seeps through. The number of nozzles can reach up to several thousand, depending on the size of the furnace. Molten glass leaves the tip of the nozzle, and as it flows down, it forms a thin fiber. The fiber is rapidly cooled below the glass transition temperature to stabilize the form with constant cool air circulation. Cold fiber then arrives at a sizing applicator. The sizing applicator applies the sizing on the glass fiber surface with minimal tension. Sizing contains various chemicals, such as coupling agents and lubricants. Sizing protects the glass fiber from environmental conditions and improves the performance of the glass fiber matrix interface. This is a heavily modifiable process depending on what type of polymer will be used as a matrix material. After the size is applied on to the glass fiber surface, the glass fiber is winded on a cylindrical collet using a winder. This collet is usually made from relatively softer materials such as paper and plastic to prevent any damage to glass fiber. The rotation speed of the winder determines the pulling speed, which determines the final fiber diameter [5, 6].

1.2.1 Production Rate of Glass Fiber

Poiseuille's formula can explain glass production. Modern facilities also use this formula to calculate the production rate of the glass fiber melting furnace. Poiseuille's formula can be seen in equation (Equation 1.1) below:

$$F \propto \frac{r^4 h}{l \times \eta} \tag{1.1}$$

In this equation, the production rate (F) is directly related to the bushing radius (r) with the orifice length (l), glass viscosity (η), and glass height above the bushing (h) [6, 13, 14]. The production rate of the glass fiber is inversely proportional to the glass viscosity. Molten glass leaves the tip of the nozzle, as it flows down the molten glass forms a thin fiber form. To stabilize the form, the fiber is rapidly cooled down below the glass transition temperature with constant cool air circulation. Cold fiber then arrives at a sizing applicator. The sizing applicator applies the sizing on the glass fiber surface with minimal tension. Sizing contains various chemicals, such as coupling agents and lubricants. Sizing protects the glass fiber from environmental conditions and improves the performance of the glass fiber matrix interface. This is a heavily modifiable process depending on what type of polymer will be used as a matrix material. After the size is applied on to the glass fiber surface, the glass fiber is winded on a cylindrical collet using a winder. This collet is usually made from relatively softer materials such as paper and plastic to prevent any damage to glass fiber. The rotation speed of the winder determines the pulling speed, which determines the final fiber diameter [3, 6, 5].

1.3 Types of Glass Fibers

Depending on the type of application that the fiber will be used, manufacturing can be relatively costly. This also creates another classification depending on the manufacturing costs of the glass fiber, cheaper being general use and expensive being the special use [15, 16]. Aside from the manufacturing costs, the main classification of glass fibers is done according to their chemical composition [17]. These different classes include E-glass fibers, which are the most common type of glass fibers, heavily dominating the market with a 90% share. The remaining 10% of the market is considered to be the special-purpose fibers [3, 14]. E-glass fibers are also divided into two different groups depending on whether they contain boron or not.

1.3.1 AR-Glass

Alkali-resistant glass fiber or AR-glass is referred to as glass fibers that have been strategically incorporated with zirconia (ZrO_2) to impart resistance to alkali ions along with improving stability [18]. The addition of zirconia into the structure of the glass fibers enhances its resistance to the potentially degrading effects of OH ions in the matrix of cement concrete [19]. The incorporation of zirconia (ZrO_2) into glass fibers serves mainly to stabilize the fiber under exceedingly alkaline conditions, with minimal impact on the intermolecular bonds between zirconia (SiO_2) and silica (SiO_2) within the fiber's structure [20]. The collaborative development of the formulation and manufacturing process of zirconia-containing alkali-resistant glass fiber was intended to satisfy thorough standards for withstanding alkaline environments. Among these compositions, alkali-resistant glass fiber with a 16% zirconia content stands out for its high resilience to the alkali environment [21]. The addition of zirconia can effectively improve the glass fiber's alkali resistance, which is a vital characteristic for the material to function well in concrete constructions. The sizing treatment applied on the fiber surface is vital, as it performs a vital role in preserving the fiber from moisture-induced damage while also improving its mechanical properties [22]. By the formation of a three-dimensional graded network on the glass surface, this treatment aids in reducing surface imperfections and increases the radius around the crack point. The sizing treatment's particular characteristics significantly affect both the tensile strength of the fiber and its ability to protect the glass surface from significant surface imperfections.

1.3.2 C-Glass

Chemical glass fiber, or C-glass Fiber, is an incredibly adaptable kind of glass fiber that finds applications in a wide variety of sectors. The main compositions of C glass fibers are 65% SiO_2, 14% CaO, 8.5% Na2O [23]. The mixture of these components gives it great chemical resistance and great electrical insulation qualities. C-glass fibers are essential in applications requiring resistance to chemical corrosion. They are widely utilized in the fabrication of chemical storage tanks and transmission lines, where their resistance to corrosive elements is critical for guaranteeing the structures' durability and strength [24]. In addition, C-glass fibers find an application in the field of electrical insulation due to their exceptional capacity to effectively insulate against electrical currents [25].This feature is critical to maintaining the safety and stability of electrical systems. The exceptional characteristic of C-glass fibers is their mechanical strength, impressive modulus of elasticity, and high tensile strength when incorporated as reinforcement components in composite materials [26]. Consequently, they are necessary in sectors that place the utmost importance on the combination of durability and flexibility. Excellent thermal stability is an additional characteristic of C-glass fibers, enabling them to cope with high temperatures without compromising their rigidity [27]. Due to this attribute, they are highly suitable for implementation in settings characterized by high temperatures, thereby enhancing their adaptability in diverse sectors. The economical properties of C-glass fibers are one of their unique features. In contrast with alternative high-performance glass fibers, C-glass fibers provide an appealing compromise between cost-effectiveness and performance. Their cost-effectiveness shows their importance in a variety of industrial sectors by making them more appealing as a sensible and affordable option for a broad range of applications.

However, C-glass fiber shows inferior mechanical properties, particularly in terms of strength and modulus (stiffness), when compared to E-glass fiber [10]. E-glass fiber is likely to be stronger and stiffer compared to the C-glass fiber. For this, the application of C-glass fiber is not commonly used in structural components of the Fiber-Glass Reinforced Polymer Composite (FGRPC). Instead, C-glass fiber is mostly used in the non-load-bearing applications of making non-structural components like building insulation materials and sewage pipes where its lower mechanical performance is acceptable.

1.3.3 D-Glass

D-glass or dielectric glass fibers are relatively uncommon in the industry compared to other types of glass fiber. They contain higher amounts of B_2O_3 compared to other types of glass fibers, resulting in a relatively lower dielectric constant than E-glass. Pure silica fibers also have much lower dielectric constant compared to the E-glass fiber. Compared to D-glass fibers, silica fibers lack the elastic modulus that is desired in the manufacturing of circuit boards. Due to the high costs of manufacturing D-glass fibers, they remain a much smaller volume compared to other fibers. Materials having very low dielectric permeabilities are frequently needed in the electronics industry. Specific volume resistance, surface conductivity, dielectric constant, and tangent of the dielectric loss angle are among the characteristics of fibers that affect their electrical properties. E-glass is typically utilized as a reinforcing filler when making boards, although the decrease in size increases the need for fiberglass in printed circuit boards. D-glasses have been graded in order to address this issue. These glasses and fibers are made using the SiO_2-B_2O_3-R_2O system as a foundation. Glasses with poor dielectric properties can contain up to 72%–75% silicon oxide and up to 20%–26% boron oxide. Alkali metal oxides, up to 3% of which are added to this solution, are used to lower manufacturing temperature. An alumina substitute can be added to silicon oxide up to 15 percent [3, 5, 6]. D-glass fibers are currently only made in limited batches due to their high cost. Furthermore, because of the high instability of this component during the charge's melting process, their high boron oxide content makes manufacturing them extremely challenging. D-glasses have a softening point of 770°C. Borosilicate glasses were designed for better electrical performance because of their low density and increased dielectric strength [3, 5].

1.3.4 E-Glass

Electrical glass Fiber or E-glass fiber was originally introduced in the late 1930s, and since then, it has been the most commonly utilized for Glass Fiber Reinforced Polymer Composites (GFRPCs) [28]. The three principal components of this category constitute E-glass fiber, which are CaO-Al_2O_3-SiO_2. However, usually, B_2O_3 and F_2 are added in percentages ranging from 0-10 weight % and 0-2 weight %, respectively, to enhance its surface quality and mitigate the formation of bubbles during the manufacturing process [11]. The production of E-glass fiber includes 7–8 weight % B_2O_3 in commercial compositions, striking a balance between melting and fiber-forming characteristics, mechanical properties, and electrical properties [29]. Commercial production of E-Corrosion Resistant (E-CR) glass fiber, which is boron-free E-glass fiber, started in the late 1970s as a proactive approach for minimizing negative environmental impacts [30]. E-CR glass fiber demonstrates remarkable resistance to corrosion in highly acidic conditions [11]. The progressive refinement of minor oxide components, including TiO_2, ZnO, and MgO, has led to the increased manufacturing efficiency and cost-effectiveness of E-CR glass fiber products. Commercially available examples of E-CR glass fiber products consist of the following: Advantex® (OCV), INNOFIBER® CR (NEG), E6 (Jushi), ECT (CPIC), and TCR [4]. Despite the progress achieved in developing low-boron compositions for general reinforcing purposes, certain sectors, like as electronics, still prefer utilizing E-glass containing roughly 6-7 weight % B_2O_3 for particular applications [4]. This preference is mostly attributed to the consistent electrical qualities and predictable processing characteristics exhibited by E-glass. The aerospace industry also demonstrates a preference for conventional E-glass fiber manufacturing methods, exhibiting hesitancy towards embracing perceived hazards even if they are low. Hence, extant E-glass fibers available in the market can be divided into two main categories: those which include low or negligible amounts of B2O3, which are necessary for general reinforcing purposes, and those featuring higher B_2O_3 percentages, whose composition was developed specifically for implementation in electronic and aerospace contexts [31]. The specific distinction between these two notions is clearly outlined according to the standards established in the ASTM D578 standard [32].

1.3.5 S-Glass

Strength glass fiber or S-glass fiber is an exceptional variety of glass fiber distinguished for its remarkable rigidity and strength. Its composition includes the following components: 55.0–79.9% SiO_2, 12.6–32.0% Al_2O_3, and 4.0–20.0% MgO [33]. The mechanical properties of this material are superior to that exhibited by other glass fibers due to the influence of these components [34]. Significantly, compared to E-glass fibers, S-glass fibers demonstrate superior tensile strength and modulus of elasticity. For applications requiring increased strength and rigidity, this characteristic renders S-Glass exceptionally suitable. Additionally, S-glass fibers are capable of being utilized in demanding environments due to their exceptional resistance to chemical corrosion, in addition to their mechanical strength [17]. This type of glass fiber is frequently utilized in the aerospace and defense industries for the production of resilient and robust aircraft components, ballistic armor, and missile casings. Furthermore, in addition to their military utility, S-glass fibers improve the functionality and strength of premium sports equipment, such as hockey sticks and tennis racquets. The comparatively elevated cost of S-glass fibers, in contrast to alternative glass fibers, is a significant factor in emphasizing their outstanding properties and specialized application.

1.3.6 Silica Glass

Silica glass fibers are primarily manufactured from silicon dioxide (SiO_2) and exhibit excellent physio-chemical properties, rendering them invaluable across diverse industrial and research applications [35]. Thermal shock resistance, spectral transmittance spanning the near ultraviolet (near-UV) to near infrared (near-IR) regions, chemical stability, electrical insulation properties, resistance to deformation upon heating, high chemical purity, and noticeable resistance to radioactive elements are some of the outstanding characteristics exhibited by silica glass fibers

[36]. Silica glass possesses these distinctive characteristics, which distinguish it from other amorphous substances. The exceptional resistance to thermal shock makes silica fiber a preferred material in industries such as telecommunications, aerospace, and automobile [37]. Additionally, the capacity for transmitting light across the near ultraviolet to near-infrared spectrum regions positions silica fiber as a key component in fiber optic communication systems and optical sensors [38]. The electrical insulating properties further enhance its utility across various applications [39]. Silica fiber stands out as a versatile and indispensable material, contributing to advancements in technology and industry. Additionally, the capacity for transmitting light across the near ultraviolet to near-infrared spectrum regions positions silica fiber as a key component in fiber optic communication systems and optical sensors [38]. The production of silica glass fiber involves various processes, including the phase transformation of natural crystalline quartz or quartz /or quartz sand, pyrolysis or /hydrolysis of $SiCl_4$, or the melting of SiO_2 gel or several other synthetic silicon compounds. According to their terms and properties, there are 4 types of silica fiber: [40].

- Type I Silica Fiber: This type of silica glass fiber is produced from natural quartz by electrical fusion under a vacuum or an inert gas atmosphere. It contains low levels of hydroxyl (OH-) groups and comparatively higher metallic impurities.

- Type II Silica Fiber: Produced from quartz crystal powder by flame fusion (Verneuille-process). It has lower metallic impurities compared to Type I, but the hydrogen-oxygen flame used in the process results in a higher hydroxyl (OH-) content.

- Type III Silica Fiber: Synthetic vitreous silicas produced by hydrolyzation of $SiCI_4$ in an oxygen-hydrogen flame. They have low metallic impurities but a high amount of hydroxyl (OH-) groups and small quantities of Cl.

- Type IV Silica Fiber: Synthetic vitreous silicas produced from $SiC1_4$ in a water vapor-free plasma flame. Similar to Type III, but with lower hydroxyl (OH-) and higher Cl content.

According to the percentage fraction of the added raw materials mentioned before, the glass fibers are classified as seen in Table 1.1.

Table 1.1: The chemical composition of glass fibers.

Compounds \ Glass Types	AR	C	D	E	S	Silica
SiO_2	58-69%	65%	72-75%	52-56%	55-80%	99.99%
B_2O_3	-	-	20-26%	6-7%	--	-
Al_2O_3	0-2%	-	0-1%	12-15%	13-32%	-
CaO	-	14%	0-1%	21-23%	22-23%	-
MgO	-	-	0.5-0.6%	0.4-4%	4-20%	-
ZnO	-	-	-	-	-	-
TiO_2	0-3%	-	-	-	-	-
ZrO_2	18-21%	-	-	0.2-0.5%	0.5-1.5%	-
Na_2O	13-14%	9%	0.4%	0-1%	0.6-1%	-
K_2O	0-3%	-	0.4%	0-0.2%	0-0.2%	-
Fe_2O_3	-	-	0.3%	0.2-0.5%	0.2%	-
F	-	-	-	0.2-0.7%	0.1%	-

1.4 Coating and Sizing of Glass Fibers

1.4.1 Sizing

Glass fibers undergo a sizing application process at the end of their production before the winding process. Applied sizing has a coupling agent present in its composition. The coupling agent is usually a silane with an organic functional group. The formula for the coupling agent can be seen below:

$$[Xi - Si(OR)_3]$$

X represents the reactive group, and R represents the methyl/ethyl group, depending on the type of the coupling agent. The silane component in the coupling agent provides protection for the glass fiber from both temperature and humidity [41, 42, 43]. In addition to these properties, silane also improves the performance of the reinforcement fiber and the resin matrix. A silane coupling agent is applied onto the surface of the glass fiber after being transformed into silanol. The silanol then creates a covalent siloxane network. [43]. After the coating of fibers is completed, the X component of siloxane is due to form a network with the resin matrix. There are different types of silanes with different X components. In this research, γ-aminopropyltriethoxysilane (APTES) is used as the coupling agent as it has been used in similar applications [43, 44].

The aim of applying the sizing is to protect the produced glass fibers from any damage right after their production. Aside from acting as a protective layer between the fiber surface and the environment, the application of sizing significantly reduces the density of the surface defects present on the glass fiber [45].

The general composition of glass fiber sizing consists of a coupling agent, a lubricant, an emulsifier, and a film former [46]. The coupling agent present in the sizing causes reinforcement fibers and the polymer matrix to have a better interface performance.

1.4.2 Effect of Coating and Sizing

It is established that the primary parameters that affect the properties of a composite material are the properties of its components. For fiber-reinforced composite materials, the properties of fiber and the properties of epoxy/resin matrix, in addition to the interface performance of these two components, are leading parameters that decide on the final properties of the composite materials. Considering the glass fiber-reinforced composite materials, the fiber design, including diameter, chemical composition, sizing, and coating (if applied), are the parameters that create the performance of the glass fiber and thus the performance of composite material [47]. One example is that the interface of the glass fiber and resin matrix is enhanced with the addition of sizing. Sizing improves the performance of the interface by increasing the strength of chemical bonding between the glass surface and bulk resin matrix [48, 49]. The effects of other nanomaterials were investigated in previous works. It was seen that carbon nanotubes were used to improve the shear strength of the glass fiber epoxy resin composite materials by coating the glass fibers with carbon nanotubes [50, 51]. The effect of nanoparticles on the performance of single fibers was investigated previously. Different nanoparticles were coated on the glass fiber surface, increasing the overall tensile strength and decreasing the failure probability of the glass fibers [43, 44].

1.5 Properties of Glass Fibers

The properties of the glass fiber composites are heavily influenced by the properties of the glass fibers and the properties of the epoxy/resin matrix. Properties of the glass fibers that compose the glass fiber composite include the fiber drawing speed, fiber diameter, fiber tex, and other parameters [17].

Fiber diameter is one of the key properties of glass fibers, heavily affecting the tensile strength of the produced glass fiber. Decreasing the diameter of the glass fiber increases the tensile strength of fibers. Increases the bending angle of the fibers. This makes fibers bendable by the guiding wheels and winders. This property is usually controlled by the pulling rate. Fiber drawing occurs with the rotational speed of the fiber winder. Increasing the winding speed results in lower diameter fibers and thus reduces the tex of the fiber. Winding speed is desired to remain constant to achieve a uniform diameter through the fiber bobbin [5].

Fiber tex is a commercially used weight-related property. It is widely used in the industry. The unit used for tex is the weight per length (g/kg). Tex of the fiber is related to the diameter of the fiber. Since the dominating parameter affecting the weight of the fiber is diameter, the fibers with a lower diameter have lower tex. The parameters that affect the diameter of the fiber ultimately affect the tex of the fiber [17].

Other parameters that affect the properties of the glass fibers include the sizing of the fiber. The oxidation of iron in the glass network heavily affects the mechanical properties of the glass fibers. The sizing protects the glass fiber from the negative effects of the environment. Iron inside the chemical composition of the glass fibers affects the viscosity, cooling, and tension [52, 53, 54, 55].

1.6 Application of Glass Fibers

Different applications of glass fibers throughout history were briefly mentioned in the historical overview section. Currently, one of the most critical applications of glass fiber comes in the form of glass fiber composites. These kinds of composite materials have a wide variety of industrial applications [23].

Currently, glass fiber is actively produced in North America, Asia, and Europe. Glass fibers are heavily used in construction and transportation fields [3].

Glass fibers are used in the construction industry in many forms. Utilizing the excellent thermal insulation properties of the glass fibers, glass fibers are fabricated in mat form to be used as thermal insulators [56]. These mats are used as wool panels and installed in between dry walls, underneath floor and roof tiling, and used as sandwich panels to provide thermal insulation for the structures.

In addition to being used as thermal insulators, the glass fiber wool is also used as a reinforcing agent for cement [57]. Similar to the epoxy/resin matrix glass fiber composites, cement is used as a matrix, and single-strand chopped glass wool is used as a reinforcement agent to increase the mechanical properties of the cement. Cement has excellent compressive strength, and the addition of glass fiber strands improves the overall strength and the fatigue performance of the cement[57, 58].

The renewable energy sector also has a growing demand for glass fiber composites. The market heavily steers to utilizing the power of wind as a clean and renewable source of energy. This creates a huge demand for mass manufacturing of wind turbines. One key component of the wind turbines, the turbine blades are constructed from the polymer matrix glass fiber reinforced composite materials. [3].

Another example is the application of laminated glass fiber composites in the marine and piping industries, utilizing the desired properties such as impact resistance, environmental resistance, and high strength. These properties are demanded to manufacture parts such as ship bodies, propellers, hatch covers, radomes, sonar covers, and other underwater equipment [59].

Polymeric glass fiber composites are also used in the aerospace industry, utilizing their lightweight and high fatigue resistance properties. One of the critical demands of the aerospace industry is the reduction of weight, making glass fiber composite one of the most promising candidates for aerospace applications [60]. Used in parts such as radomes, landing gear covers, and other plate-shaped parts. Other than that, the glass fiber composites also utilize the thermal insulation properties of the glass fibers. Using them as insulator panels on rockets and spaceships.

Leading factors in the utilization of glass fiber composites in the aerospace industry are the high acquisition and the cost-effectiveness of the autoclave systems in glass fiber composite production. Also, the demand to reduce the weight of the aircraft, which directly affects fuel efficiency, is also one of the factors that has increased the demand for glass fibers. The use of glass fiber composite materials in the aerospace field improved overall safety and fuel economy. The strength-to-weight ratio and mechanical performance of the glass fiber composites made them excellent constructional elements for both the interior and exterior components of the aircraft. Using glass fiber reinforced composites on parts where conventionally metals such as aluminum are used provided significant weight reduction [17].

Currently, glass fiber composites are used as secondary structural components on aircrafts. These components are usually fairings, wing tips, and radomes. Glass fibers are utilized in radomes for their low dielectric constant, which provides high signal transmittance in X-Band signals [61, 62].

1.7 Intrinsic Flaws of Glass Fibers

The strength of the glass fiber is one of its key properties that makes it such a versatile material used in many applications such as aerospace and automotive. There are many parameters that affect the overall strength of the glass fiber. The manufacturing process, chemical composition, type of sizing used on the final product, and thermal history are some of the parameters affecting the strength of glass fiber. Depending on the optimization of the manufacturing process, from the raw materials used to the final application of the sizing, the strength can be improved.

1.7.1 Griffith's Flaw Theory

Griffith's Flaw Theory aims to understand how and why a fiber breaks at specific tensile strength. In 1920, Griffith came up with a theory that explained the failure behavior that the glass fibers exhibit [63, 64, 65]. In the context of this, there are two different formulations regarding the glass fiber behavior.

One of these formulas shows the relation between the size and the strength of the glass fiber sample. In the context of glass fibers, the term size is considered to be the length of the fiber. The theory explains that glass fibers intrinsically have flaws, such as cracks and variations of diameter, that form through their fabrication process. If the length of the fiber increases, the probability of such a flaw to be present on the sample increases. This ultimately results in a decrease in the overall tensile strength of the glass fiber sample.

In this concept, the presence of defects in the glass fiber is already established. These defects are also considered to be the concentration point of the applied stresses, whether they are on the surface or inside the bulk of the fiber. For a fiber to reach the point of failure, the defect has to propagate to a critical length. Griffith explained the calculation of the maximum stress that fiber can withstand, as seen in equation (Equation 1.2) below:

$$\sigma_f = \sqrt{\frac{2E\gamma}{\pi \times c*}} \tag{1.2}$$

In this equation, the maximum failure stress (σ_f) of a glass material can be calculated with the Elastic Modulus (E), interfacial surface energy (γ), and critical depth length of crack (c*) of the sample. The relation between the actual strength value is heavily dependent on variables such as Elastic Modulus and interfacial surface energy, which both are driven by the chemical composition of the glass material [63, 64, 4]. In addition to defects, moisture can heavily affect the final strength value of the glass fibers with a decrease.

1.8 Analysis of Statistical Strength

Glass is considered a brittle material. Therefore, glass fibers are also brittle. Brittle materials have a wider range of distribution considering their tensile strength values. This is mainly caused by their intrinsic flaws, and for calculation statistical approach is applied [66]. Materials are deemed to break at their weakest points. The flaws mentioned before act as stress concentration points and cause materials' overall tensile strength to decrease significantly. Weibull Distribution is a statistical method that is the preferred approach in calculating the strength values of brittle materials as it is coherent with this type of application. It is a failure of the "weakest link theory" based distribution function. This theory is based on several assumptions. It assumes that failure starts at the "weakest link", which in the concept of this study, the intrinsic flaws of fiber and other flaws do not have any effect over this weakest point [45, 64]. It is also assumed that the strength of the material is a time-independent variable, and the flaws present in the material are independent of each other, and material failure is dependent on a single flaw. Weibull distribution defines the probability of failure of a brittle material as:

$$P = 1 - \exp\left[-\left(\frac{\sigma_f - \sigma_u}{\sigma_0}\right)^m\right] \tag{1.3}$$

In this equation, the probability of failure is defined as P, failure strength is σ_f, threshold strength is σ_u, the scaling parameter is σ_0, and the Weibull modulus is m. The scaling parameter is heavily dependent on the number of samples and their strength rankings. Threshold strength is the threshold stress value for a fiber to fracture, meaning it is not possible for a fiber to fracture below that stress value. Weibull modulus defines the scatter of the data. In the case of this study, the parameters are the actual tensile strength values of the sample group. The Weibull modulus is desired to be increased, meaning the Weibull plot has a greater slope so the data is less scattered, and there is less deviation. This can be interpreted as if the Weibull modulus is high, the probability of failure of that sample group is low. Assuming that there is a possibility of fibers being fractured before they are tested, the threshold strength can be considered as 0. With this assumption, a new equation can be formulated as:

$$P = 1 - \exp\left[-\left(\frac{\sigma_f}{\sigma_0}\right)^m\right] \tag{1.4}$$

Another important assumption for this statistical approach is that fiber fracture is attributed to a single flaw in the glass fibers structure [67]. In order to get the Weibull modulus value, the slope of the Weibull plot for the data group is obtained through the following equation:

$$ln(ln(\frac{1}{1-p})) = mln(\sigma) - mln(\sigma_0) \tag{1.5}$$

In addition to this equation, to calculate the failure probability of the glass fiber sample group following equation is used:

$$P_i = (\frac{i - 0.5}{N}) \tag{1.6}$$

Here the probability of failure is P_i, and N is a scaling factor depending on the ranking of fracture stress value in the sample group [68].

1.9 Fractography

When fibers are characterized for their mechanical properties, sets of tests are generally destructive. The tensile testing method is used to collect data on the strength of a single fiber. Tensile stress is applied to the sample until critical failure stress is reached and the fiber is fractured. There is a characteristic fracture surface form for fibers, which can be seen in the figure.

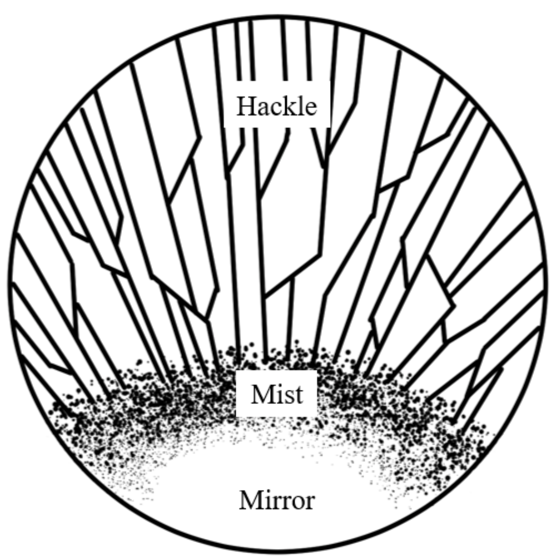

Figure 1.3: Schematic representation of the cross-section of glass fiber fractured by tensile force, indicating mirror, mist, and hackle region [56].

Fractured glass fiber cross-section can be divided into three different sections:

hackle, mist, and mirror region. Hackle region can be described as the most extensive and roughest region in terms of texture. The mist region is the transition region between the hackle and mirror regions. The mirror region is the smoothest, and it is also the starting point of the fracture. The sizes of these regions and the tensile strength of the glass fiber can be formulated as follows:

$$\sigma_f = \frac{A_m}{\sqrt{r_m}} = \frac{A_h}{\sqrt{r_h}} \tag{1.7}$$

In this equation, failure stress is σ_f, mirror and mist region is r_m, and mirror hackle region is r_h. A_m and A_h are the constants whose values are (1.7-1.9) and (2.0-2.1), respectively [69, 70, 71].

1.10 Objective

The overall tensile strength of the glass fibers is dependent on factors such as the chemical composition of the glass, fiber dimensions, stress history, flaws, thermal history, and atmospheric conditions [43, 55, 72, 73]. This thesis aims to investigate further the effect of nanoparticle doping on the E-glass fibers. From the predecessors of this work, nanoparticles can be used to improve mechanical and chemical properties of the E-glass fiber [43, 44]. In the previous sections, it has been established that the fibers intrinsically have flaws present on them from the moment they were fabricated. These flaws decrease the strength of the fibers drastically, which is highly undesirable. By utilizing the nanoparticles, the decrease in strength can be minimized with a relatively cost-efficient and easy-to-integrate method.

In this thesis, the effect of ZnO nanoparticles on the E-glass fiber's mechanical, chemical and electromagnetic properties will be investigated. Weibull distribution and statistical approach are taken to investigate the effect of the coating on the overall tensile strength properties of the glass fibers. After that, the performance of fibers will be investigated by exposing glass fibers to an acidic environment.

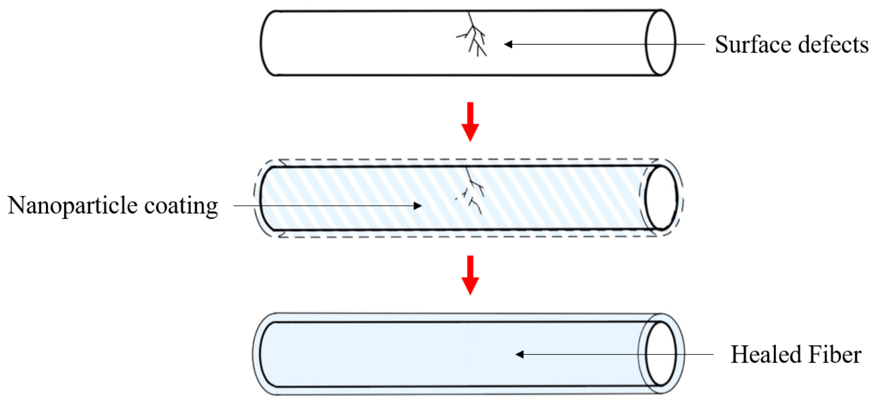

Figure 1.4: Schematic representation of glass fiber coating process.

The fiber surface will be investigated to uncover the effects of nanoparticle coating. Finally, the final product is aimed to be a glass fiber composite; therefore, the other effects of nanoparticle coating, such as electromagnetism, will be investigated in composite application.

In addition to nanoparticle coating of E-glass fibers, a specialized silica fiber is aimed to be fabricated with a novel method. The objective of developing a new method to fabricate the silica fiber is to offer a cost-effective alternative to current structural silica fabrication method by changing the heat source of the system and making the draw tower comparably compact to the alternative drawing systems.

Chapter 2

Experimental Methodology and Procedure

2.1 Methodology

In the experimental section, custom E-glass fibers produced and supplied by SISECAM A.Ş. and the sizing silane coupling agent (APTES) were used. ZnO nanoparticles were sourced from Nanografi, Turkiye. The glass fibers were doped using these nanoparticles and coupling agents and then heat-treated. After the preparation, the samples were characterized using various mechanical, chemical, electrical, and spectroscopic characterization methods. For mechanical characterization, a micromechanical tester (Instron 6700 series) was used. Fibers were exposed to an acidic environment for chemical characterization and then characterized through Environmental Scanning Electron Microscopy (E-SEM). Finally, various characterization methods through Energy Dispersive X-ray spectroscopy (EDX), X-Ray Diffraction Analysis (XRD), X-Ray Photoelectron Spectroscopy (XPS), and Zeta Sizer were used to characterize the samples and raw materials used to prepare the samples.

2.2 Sample Preperation

2.2.1 Preperation of Single Fiber Test Samples

Samples are prepared through multiple steps. These steps include keeping fibers under vacuum and resizing them to be able to fit inside the sample holder, preparation of different ZnO nanoparticle solutions (5%, 7.5%, 10%, 12.5%, and 15%), preparation of silane solution (1%), preparation of sample holder, two-step dip coating process, attachment of fibers to the sample holder.

SISECAM Inc.-supplied E-glass fibers are resized to approximately 70 mm in length. This is done to decrease the slipping by increasing the interface between the glue and the fiber surface. Fiber diameters were measured to be between 50 to 60 μm using an optical microscope prior to any testing. Zinc oxide nanoparticle solution 22 w% water dispersion solution from Nanografi, Turkiye was used to prepare 5%, 7.5%, 10%, 12.5%, and 15% solutions through dilution using DI water. APTES solution is also prepared by diluting a pure APTES to a 1% solution using DI water. Both ZnO nanoparticle and APTES solutions were gone through ultrasonication to achieve a homogeneous solution. Bare fiber samples are used as the control group. Bare fibers were dipped into DI water to imitate the same procedure the ZnO-coated fiber goes through and compare the effect of nanoparticles.

Figure 2.1 describes the total process of sample preparation and micromechanical analysis. The fibers are resized according to the size of the sample holder. The sample holder has an opening that is 25 mm in length. However, fibers are resized to approximately the same length as the sample holder to achieve a larger fiber-glue interface to reduce the slippage. Fibers are coated with ZnO nanoparticles via dip-coating method, and bare fiber is dipped in DI water to act as a control group. After dip-coating, fibers are carefully placed in a vacuum furnace at 120 °C. The annealing process takes 30 minutes under vacuum to remove any humidity from the samples and create optimal conditions for chemical bonding.

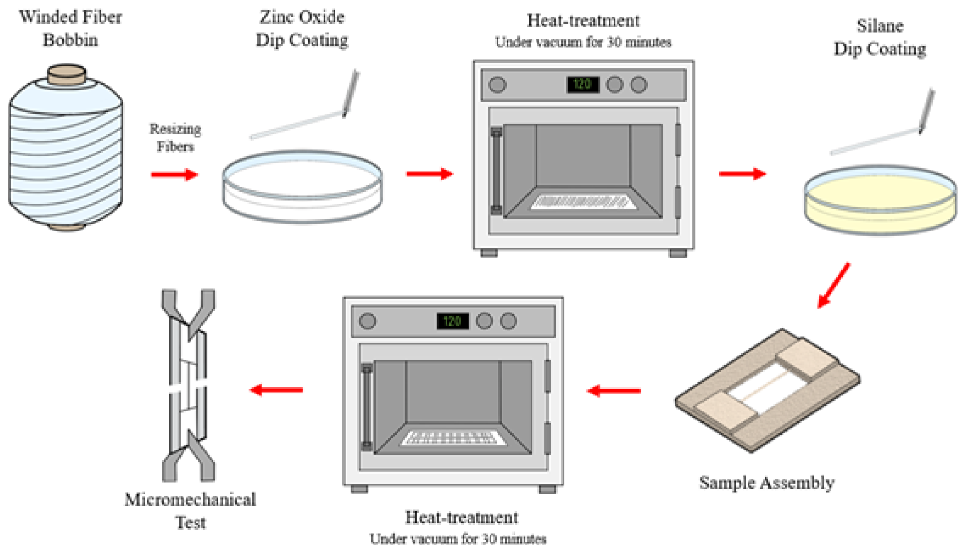

Figure 2.1: Schematic diagram illustrating the sample preparation process for the tensile test.

After annealing is completed, both nanoparticle-coated and bare fibers are dip-coated with 1% APTES solution. APTES is used for multiple reasons, including hydrothermal resistance and better glass fiber reinforcement matrix interface performance [41]. After all the samples were coated with APTES solution, they were placed in the vacuum furnace at 120 °C for another 30 minutes. After this, fibers are mounted on the custom frame-shaped sample holder using a polymer-based glue.

2.2.2 Preperation of Acid Test

The acid test is conducted on 10 % ZnO nanoparticle-coated fibers. Acid tests were conducted after the mechanical tests; therefore, only the 10 % concentration solution was tested. The sample preparation procedure was similar to the tensile test sample preparation, as seen in Figure. Samples were coated with 10 % ZnO nanoparticle solution using the dip-coating method. After that, the fibers were placed inside the vacuum furnace at a 120 °C temperature for 30 minutes. This is done to remove any moisture that is present in the samples. After that, the nanoparticle-coated fibers were dip-coated again to the 1% APTES solution. For the preparation of the bare fiber samples, the same procedure was followed by replacing the 10 % ZnO nanoparticle solution with DI water. Both sample groups were placed on the custom sample holder to be submerged in the acidic environment. A 37 % fuming HCl solution was used to create an acidic environment with a pH of 1 (20 °C) for 24 hours. After that, the glass fiber sample surface is inspected using Environmental Scanning Microscopy.

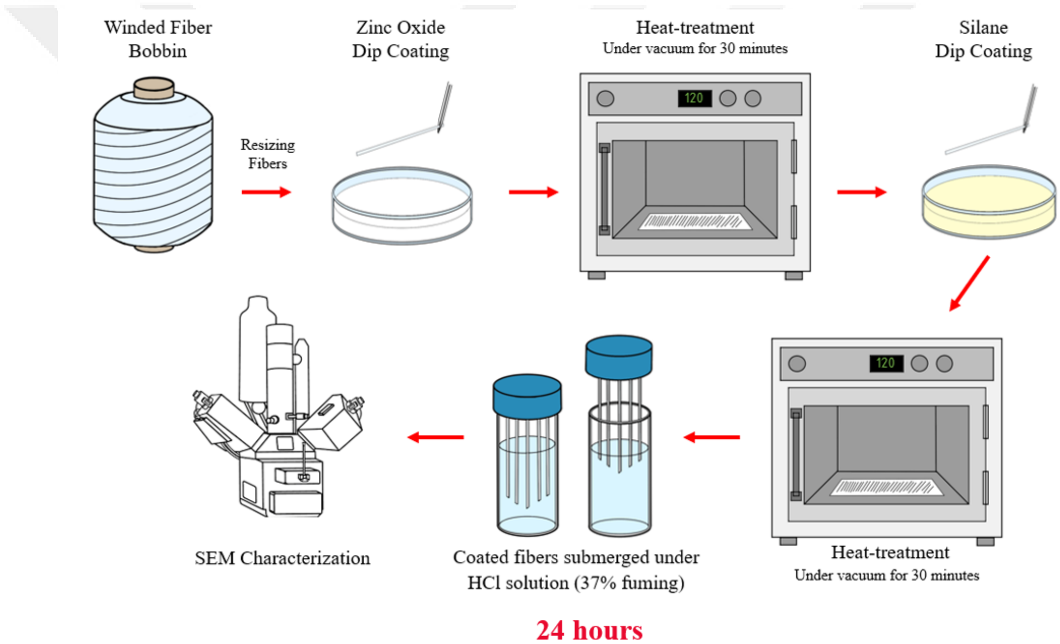

Figure 2.2: Schematic diagram illustrating the sample preparation process for the acid tests.

2.2.3 Preperation of Glass Fiber Felt Composite

A composite sample is prepared to investigate the effect of ZnO nanoparticle coating of fibers on the overall dielectric properties of the composite material. As a first step, a 3D CAD model for the composite sample with specific dimensions is designed using SolidWorks CAD software. Dimensions are determined for the sample to be able to fit inside the Keysight Network Analyzer E5063A sample holder. For accurate results, the sample must fit snugly into the sample holder with no empty space. CAD model is made using SolidWorks CAD software and a mold is designed for a silicone mold that the composite sample will be made into. The first mold is made from PLA material using Creatlity Ender V2 3D printer. Then RTV-2 molding silicone is used to create the mold for the composite sample. With the production of silicone mold, the preparation of bare glass fiber felt, and ZnO nanoparticle-coated fiber felt started. Similar to the single fiber coating process, the fibers are coated with DI water and 10% ZnO nanoparticle solutions. Then annealed in a vacuum furnace for 30 minutes to remove any water from the fiber surface. Then both sample groups are dip-coated with a 1% APTES solution. After being annealed again in a vacuum for 30 minutes, the fibers are removed. Prepared fibers are chopped into smaller pieces and placed into the silicone molds. A commercially available epoxy resin is poured onto the molds to create a glass fiber felt-reinforced epoxy resin matrix composite. Molds are put under a vacuum to remove any bubbles that may trap inside the resin matrix. After the samples are prepared for the exact dimension to fit inside the Keysight Network Analyzer E5063A.

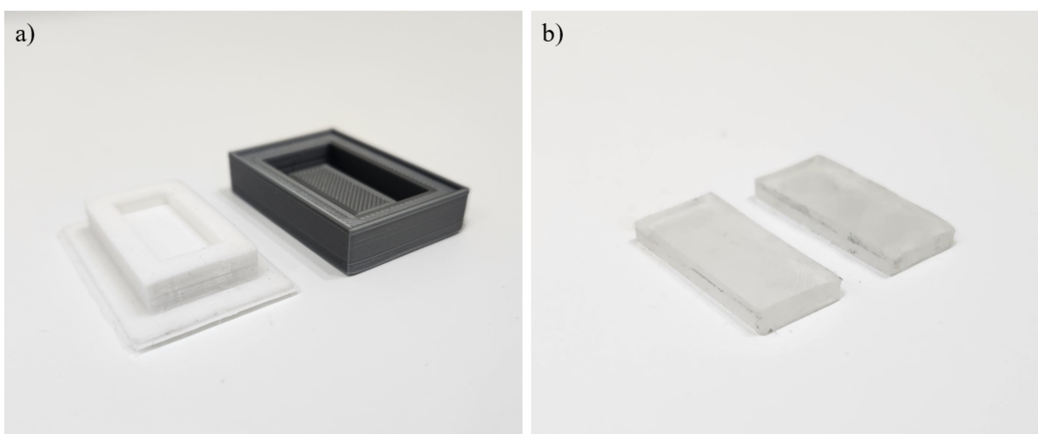

Figure 2.3: Images of a) Casted silicone (left) and 3D printed PLA (right) mold for preparation of composite samples and b) fabricated glass fiber felt composites

2.3 Characterization of Samples

2.3.1 Micromechanical Analysis

Tensile strength calculation requires material to be put under critical stress to cause its failure. Tensile strength analysis requires a micromechanical analyzer to test the glass fiber samples. In this study, an Instron 5960 Micromechanical Analyzer is used. The test parameters were defined as 1 mm/min extension rate according to ASTM D3832M-14 [47]. Since the fiber diameters are not equal through the length of a fiber batch, the average diameter of fibers was measured, calculated, and set as 60 μm using the ZEISS AX10 Optical Microscope. This is done to reduce the time required for the testing process. After the testing was completed, the actual diameters of the remaining fibers after elimination were measured using the same optical microscope. Actual tensile strength values were recalculated with actual diameter values. Fibers are attached to the frame-shaped sample holders. Holder dimensions are set to be 75 mm in length and 55 mm in width. Frame opening is set to be 25 mm in length and 35 mm in width. These dimensions were determined considering the micromechanical analyzer's sample holder jaws. A frame-shaped sample is placed on the micromechanical tester using the jaws present on the tester. Sidebars are then severed so that when the stress is applied to the sample, the only structure that is exposed to the stress is the single fiber strand. There were different fiber fractures seen during the testing session. Only the data of middle fractured fibers were accepted since the cause of the fracture is only the tensile stress. Fibers that broke on the edge of the sample holder and gone were disregarded since the fibers fractured on the edge might fracture due to the interaction of the fiber and the sample holder. Middle-broken fibers are considered reliable samples, and their tensile test data are considered acceptable. Each sample group had 100 fibers, 50 bare fibers, and 50 ZnO-coated fibers. The average middle fracture turnout rate for the samples was approximately 60% making the average number of acceptable fiber data 30. Using 30 different samples for each subgroup provided a data accuracy of around 96% [43]. Since the diameters of glass fibers are not the same for the samples, the diameter of the fibers is individually measured using a ZEISS AX10 Optical Microscope. A tensile test was conducted, assuming all the fibers have a 60 μm diameter. By using the same formula for stress:

$$\sigma = \frac{F}{A} \tag{2.1}$$

In this equation, σ is the stress, F is the force, and A is the cross-sectional area of the glass fiber. From the micromechanical test, the maximum force before the glass fiber fracture can be obtained through calculations. Assuming the fiber diameter to be 60 μm, resulting in a constant cross-sectional area in calculations of the micromechanical tester. In order to obtain the actual tensile strength of the fiber, information on cross-sectional area is required and can be obtained via the following equation:

$$A = (\pi d^4)/4, \tag{2.2}$$

Using this equation, the actual diameter of the fiber can be measured using a microscope and replaced with the assumed diameter of the glass fiber to obtain an accurate value of the tensile strength of the fibers.

Actual diameter values are used in the statistical analysis to observe the effect of ZnO nanoparticles on the mechanical properties of the glass fibers. Actual tensile strength value of the sample is considered to be the failure strength in the following equation:

$$P = 1 - \exp\left[-\left(\frac{\sigma_f}{\sigma_0}\right)^m\right] \tag{2.3}$$

2.3.2 Scanning Electron Microscopy

Scanning Electron Microscopy (SEM) is used to characterize the quality of the fiber surface, the quality of the ZnO nanoparticle coatings, and the after-effects of the acid test on the glass fiber surface. This type of microscopy utilizes the electrons that are launched by the electron gun present in the SEM. The electrons interact with the sample and result in secondary electrons, back-scattered electrons, and x-rays. These provide information on the surface features and elemental compositions of the sample. SEM requires the sample to be conductive to generate the images of the sample. In order to obtain high-quality images of the glass fiber surface, which is an electrical insulator, the samples are coated with a 10 nm layer of gold and palladium using a Precision Etching Coating System (PECS). Using these coatings, the surface images of 5%, 10%, and 15% ZnO Nanoparticle solution coating were obtained without charging the samples and distorting the images.

2.3.3 Energy Dispersive X-Ray Spectroscopy

Energy dispersive X-ray spectroscopy (EDX) is used to characterize the elements on the sample surface. It utilizes the X-rays and excitation caused by the X-rays. Each element possesses a certain peak value on the electromagnetic emission spectrum. The x-rays are sent onto the sample, exciting the ground state electron on the sample. Creating an electron hole, an electron from the outer shell moves and fills the hole resulting in the difference in energy, emitting an X-ray. The energy values are obtained through the difference in the energy. EDX is used to characterize the coating on the glass fiber surface and create an elemental mapping on the glass fiber images.

2.3.4 X-Ray Photoelectron Spectroscopy

X-ray photoelectron spectroscopy (XPS) is a characterization method that utilizes the photoelectric effect of the materials. It is based on the energy emission from the excited electrons, excited by an incident X-ray photon. Each excited electron emits a characteristic amount of energy depending on which element and which electron band the excited electron resides. The intensity of the peaks obtained is related to the amount of atoms that element in question is present on the characterized sample. Every single element has a characteristic binding energy which is used to characterize the specific elements present on the sample that is being characterized. XPS can detect almost every element except hydrogen and helium.

2.3.5 Network Analysis

Network analyzer is the instrument of choice for measuring network parameters of electrical networks by providing basic measurement technology in RF and microwave industries. It is also preferred for design evaluation and testing of active and passive electronic components. With this instrument, transmission and reflection measurements are performed, and the results obtained are evaluated. The basic working principle of the device is to measure the phase and amplitude of both waves, reflected and incident waves, at different ports of the device under test. It includes both a receiver and a source set. The source set is used to generate a known excitation signal, while the receivers are used to examine changes in the excitation signal caused by the device under test. The analysis takes place ten minutes after the configuration change. The measurements are grouped into scattering, reflection, and transmission parameters. The transmission parameter is used to determine insertion loss, gain, and transmission coefficient, while the reflection parameter is used to determine the reflection coefficient, impedance, and return loss. The scattering parameter is used to analyze the s-parameters [62].

Chapter 3

Zinc Oxide Nanoparticle Coated E-Glass Fibers

3.1 Introduction

Glass fibers are heavily used as reinforcement materials in fiber-reinforced composite applications, dominating the market with a 95% share [6, 3]. Exploiting their mechanical properties, such as a high strength-to-weight ratio, low thermal expansion, and high-impact resistance, glass fibers are used in numerous industrial fields such as aerospace, construction, thermal and sound insulation, and renewable energy [28, 74]. Over the years, various types of glass fibers with different chemical compositions have been developed depending on the applications. Among these types, E-glass fiber is heavily used, supplying the majority of the market demand [6].

Glass fibers are preferred over other types of reinforcement fibers due to their cost efficiency and high strength-to-weight ratios [41, 43, 74]. Improving the mechanical performance of the glass fiber reinforcement will lead to an improved glass fiber composite final product. The introduction of different metal oxide nanoparticles to the surface of the glass fibers leads to improved mechanical and chemical properties. Previous work proved that this concept is achieved through the TiO_2 and ZrO_2 nanoparticle coatings [43, 44]. Metal oxides used in fiber coating improve the fiber and matrix interface performance. Metal oxides are already present in the chemical composition of glass fibers. The different nanoparticles were referred to according to their different applications.

The acid resistance of fibers is important regarding the environment of the application. Zinc Oxide has previously been used in acid-resisting applications on metals and rubbers [75, 76, 77]. Corrosion on the glass surface is unwanted due to the formation of cracks and deformation. These acid-induced surface defects significantly reduce the mechanical properties of glass fibers by inducing stress localization.

Further investigating the effect of nanoparticle concentration on the quality of the coating, different concentrations of ZnO nanoparticle coating were used. Different naming conventions for the different sample groups can be seen in Table 3.1. In previous works, the sample groups were limited to Bare fibers, 5%, 10%, and 15% nanoparticle coatings. In order to have more accurate data and confirm the optimum nanoparticle solution concentration, the sample groups are increased to Bare Fiber, 5%, 7.5%, 10%, 12.5%, and 15% ZnO nanoparticle solutions. Sample group names can be seen in Table 3.1.

Table 3.1: Names used for different types of ZnO nanoparticles-coated fibers.

SAMPLE TYPE	DESCRIPTION
BF	Bare fibers (0% ZnO nanoparticle-coated fibers)
5ZNCF	5% ZnO nanoparticle-coated fibers
7.5ZNCF	7.5% ZnO nanoparticle-coated fibers
10ZNCF	10% ZnO nanoparticle-coated fibers
12.5ZNCF	12.5% ZnO nanoparticle-coated fibers
15ZNCF	15% ZnO nanoparticle-coated fibers

3.2 Results

3.2.1 Characterization of Zinc Oxide Nanoparticles

Zinc oxide nanoparticles were purchased from Nanografi, Turkey. The data sheet claimed that the nanoparticles have a size range of 25 to 35 nm. The nanoparticles came in a 22 w/% water-dispersed nanoparticles form. In order to confirm that the received nanoparticles were indeed ZnO, the X-ray Diffraction analysis was conducted. The results of the XRD can be seen in Figure 3.1. The sharp intensity peaks that are visible come from the (100), (002), (101), (102), (110), (103), (200), (112), (201), (004) and (202) planes of the characterized nanoparticles. The peaks obtained from the scan coincide with the characteristic peaks of the hexagonal wurtzite crystalline structure of zinc oxide.

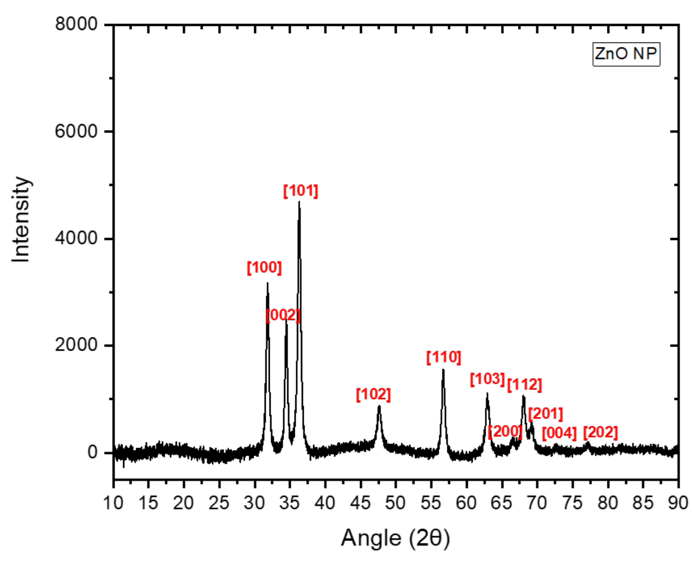

Figure 3.1: XRD results of ZnO nanoparticles

To further characterize the nanoparticle solutions, 22% and 5% solutions were taken to the Zeta Sizer. A hydrodynamical size distribution analysis was conducted to confirm the stability of the nanoparticle solution. The size distribution measurements were taken at different time intervals. Through different time intervals, the hydrodynamical size peaks remained constant for both solutions. It can be concluded that the nanoparticles do not clump over time, and the solution is stable. It was mentioned on the data sheets that the nanoparticle sizes are 25 to 35 nm. This was confirmed using a Scanning Electron Microscope.

3.2.2 Spectroscopic Analysis

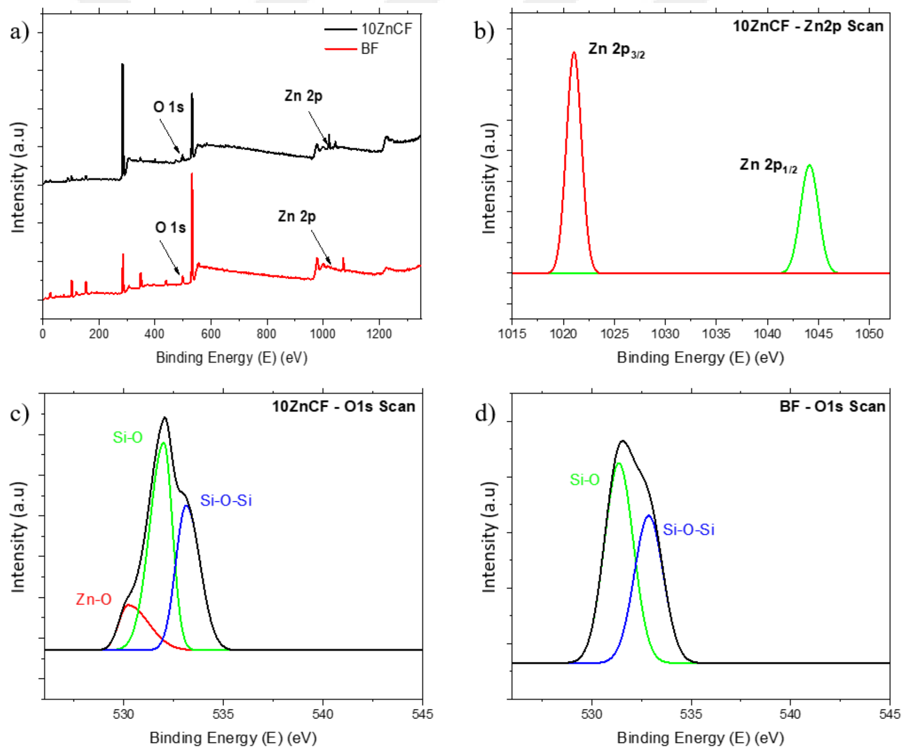

Figure 3.2: XPS spectra measurement showing a) full spectra of BF and 10ZnCF, b) Zn2p scan of 10ZnCF, c) O1s scan of 10 ZnCF, and d) O1s scan of BF

X-ray photoelectron spectroscopy and energy-dispersive X-ray spectroscopy were conducted on the coated and bare fibers. In Figure 3.2, the bare fiber and 10% ZnO nanoparticle-coated fiber spectra are seen with a slight Y offset. The visible peaks on the 1022 eV and 1043 eV are from the zinc 2p scan. Comparing these two spectra, the peaks from the zinc 2p scan are clearly visible compared to the bare fiber. Comparing the sample spectra, it is clearly visible that the

10% coating has distinctive Zn 2p peaks compared to the literature [78]. The nanoparticle coating percentage affects the intensity of the coating. With increased nanoparticle concentration on the glass fiber surface, the peak intensity increases [44]. The presence of ZnO nanoparticles on the glass fiber surface is confirmed.

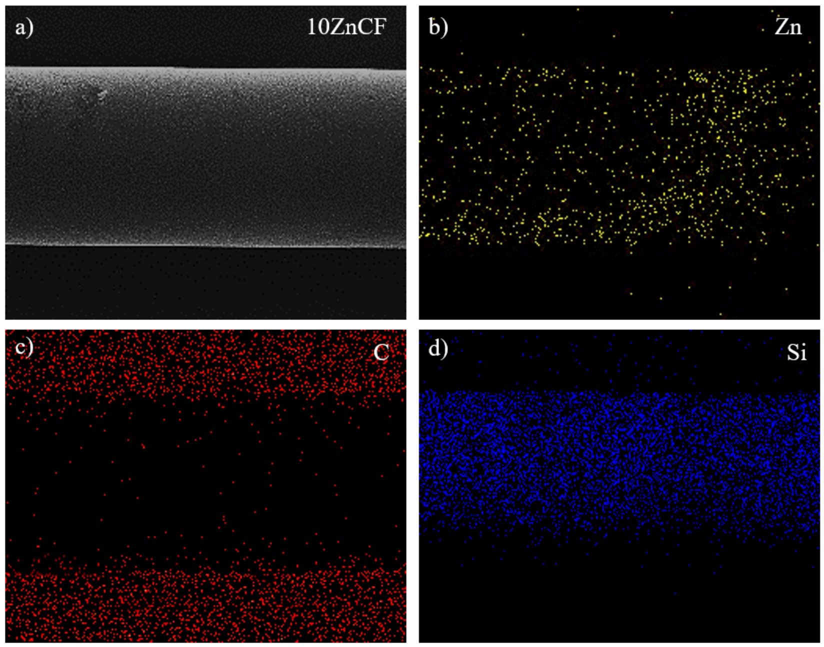

Figure 3.3: Zn, C, and Si elemental mapping of 10% ZnO nanoparticle coated fiber.

In Figure 3.3, the elemental mapping for the 10% ZnO nanoparticle-coated fiber is visible. The surface of the fiber is coated with a uniform monolayer of ZnO nanoparticles. Therefore, the yellow coloring on the surface on the map is from Zinc. The samples were placed inside the scanning electron microscope by attaching them to carbon tape. Carbon readings are from the carbon tape that the fiber is attached to. Silicon readings are from the surface of the glass fiber. The scarcity of the zinc signal could be attributed to the coating thickness being a monolayer of ZnO nanoparticles.

3.2.3 Morphological Analysis

Morphological analysis is conducted using the Environmental Scanning Electron Microscope. In order to compare the quality of coating for different nanoparticle solution percentages, the bare and coated glass fiber surface images are taken. Figure 3.4 shows the difference in coating quality for different nanoparticle solutions.

In Figure 3.4 and 3.5, the glass fiber surface is smooth. The surface is coated with ZnO nanoparticles. The coating is not uniform for 5ZnCF and 7.5ZnCF sample groups. The surface of the glass fiber is clearly visible through the empty spaces of nanoparticle coating. Uniformity of coating is important and is seen to affect the improvement of the mechanical properties of glass fibers [43, 44]. The same happened with the 7.5ZnCF sample group; the population of the nanoparticles increased but a uniform coating was not achieved. The best results were obtained from the 10ZnCF sample group. The glass fiber surface is uniformly and fully coated with a single layer of nanoparticles. For the 12.5ZnCF sample group, the coating started to lose its uniformity, and the coating became thicker. Evaluating the 15ZnCF sample group, the surface is coated with a thick layer of ZnO nanoparticles. The uniformity decreased increasingly after the concentration of nanoparticle solution exceeded 10%. There were visible defects induced by the clumping of nanoparticles in certain locations. These defects can act as stress localization points and decrease the overall performance of the glass fibers.

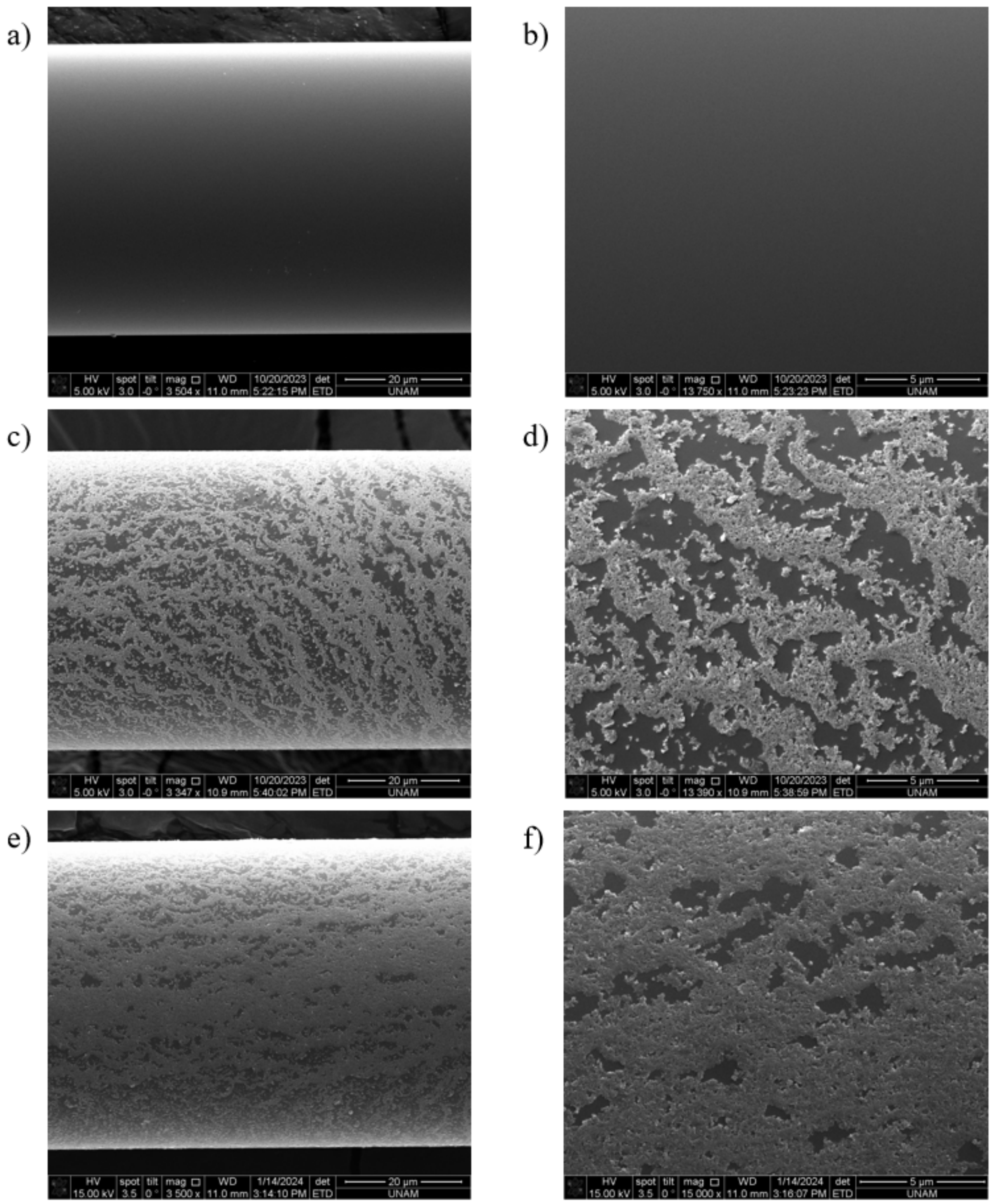

Figure 3.4: SEM images of a) BF, b) BF surface, c) 5ZnCF, d) 5ZnCF surface, e) 7.5ZnCF, and f) 7.5ZnCF surface.

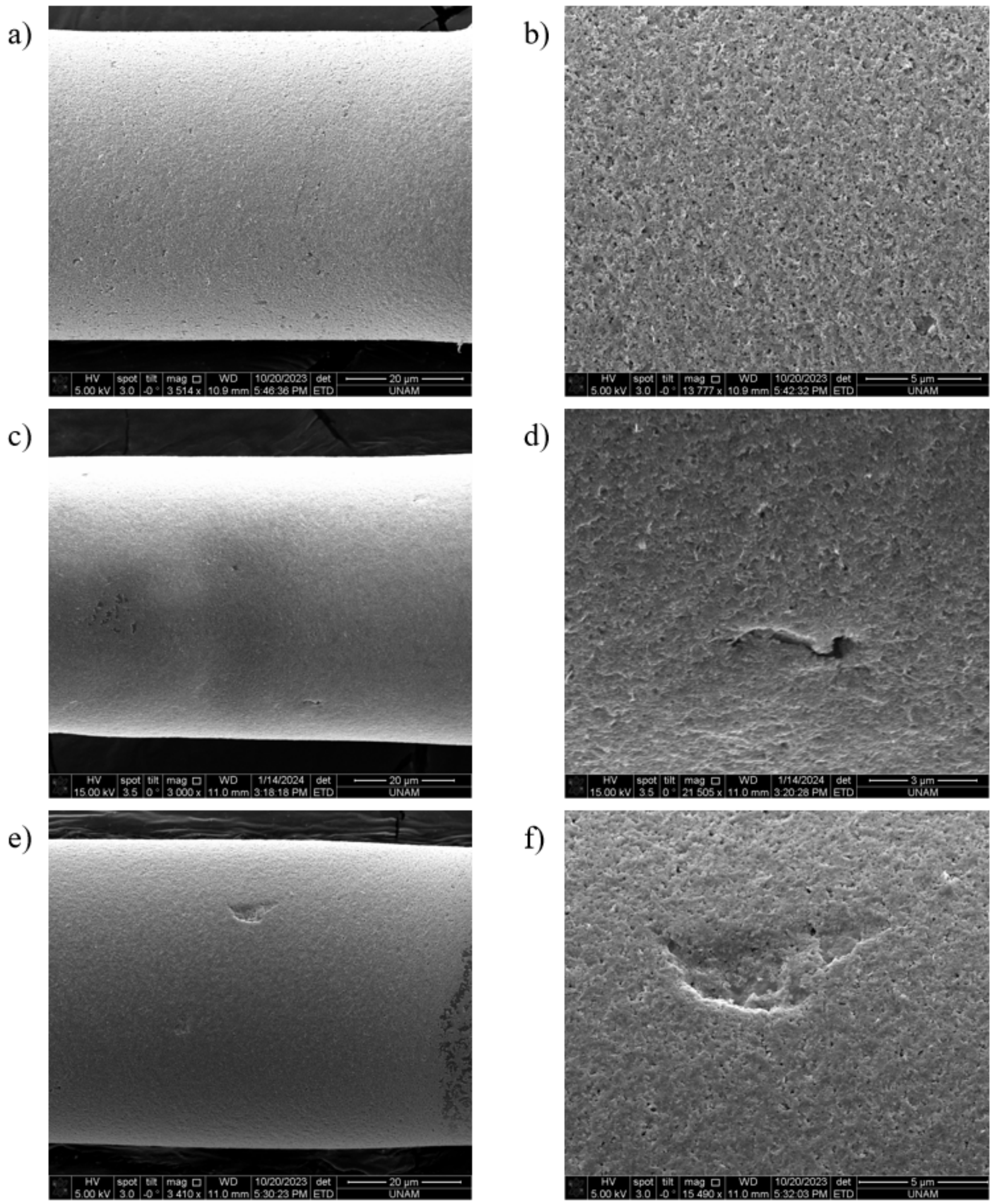

Figure 3.5: SEM images of a) 10ZnCF, b) 10ZnCF surface, c) 12.5ZnCF, d) 12.5ZnCF surface, e) 15ZnCF and f) 15ZNCF surface

3.2.4 Fractrographic Analysis

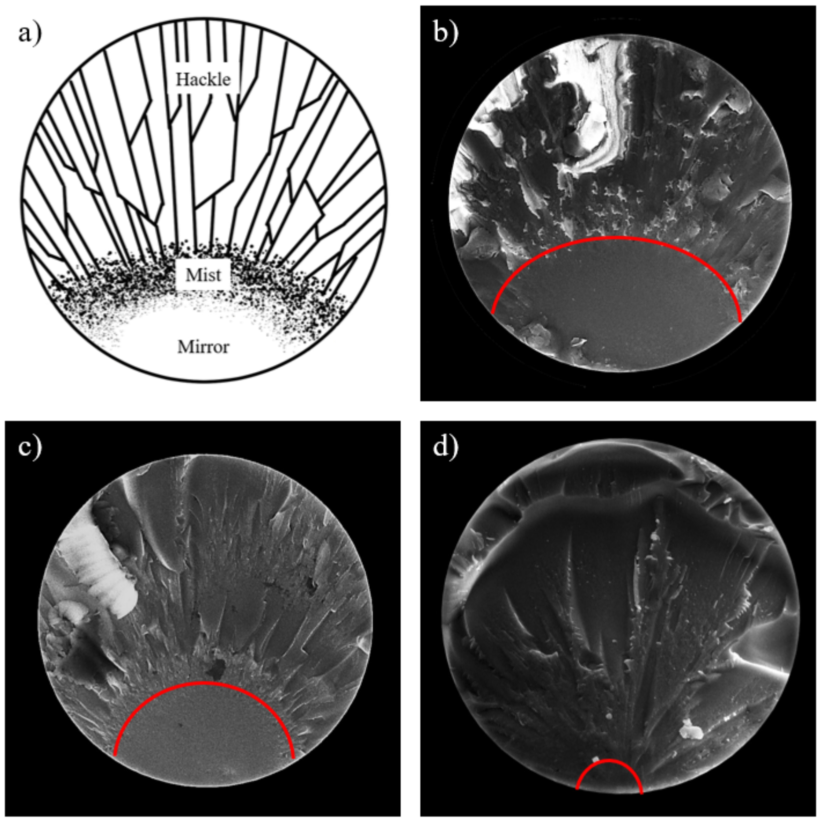

Figure 3.6: a) Schematic representation of the cross-section of glass fiber fractured by tensile force, indicating mirror, mist, and hackle regions and SEM images of fracture surfaces of glass and fibers with tensile strength values of b) 711, c) 1061, and d) 1827 MPa.

The fracture surface of the glass fibers that underwent the micromechanical test was investigated under the scanning electron microscope. Figure 3.6 compares the cross-sectional image of the fractured fibers and their tensile strength values. As the tensile strength of the fiber increases, the area of the characteristic mirror region of the fiber decreases. When comparing the fibers with tensile strength values, the fiber with the highest tensile strength value of 1827 MPa has the smallest mirror region area. This trend is not affected by the nanoparticle coating and is seen as consistent. The presence of a characteristic fracture surface profile confirms the fibers were broken solely due to the tensile stress.

3.2.5 Mechanical Analysis

ZnO nanoparticle-coated E-glass fibers are tested using a tensile testing machine to investigate the effect of nanoparticle coating on the overall strength of the glass fibers. Fibers are coated with different concentrations of ZnO nanoparticle solutions. 5%, 7.5%, 10%, 12.5%, and 15% concentrations of nanoparticle solutions were used to coat the fiber surface.

Morphological analysis results show that each solution coated the fiber surfaces, resulting in homogeneous surface coverage in some cases. It can be assumed that the nanoparticles cover and repair any defect present on the glass fiber surface. This can also be related to the formation of a polysiloxane network from the interaction between the coupling agent and nanoparticles [41, 43, 67]. In order to increase the statistical reliability of the tensile tests, each sample group includes 50 fiber samples. During the micromechanical test, fibers that broke on the sample holder edge and samples that slipped were removed from the data group to increase the accuracy of the data. After the elimination of unacceptable samples, the remaining samples were approximately 30, with a turnout rate of 60%. 30 samples provide an accuracy of 96%, which is acceptable for a statistical approach. The tensile strength of the fibers differs due to multiple factors. The atmospheric conditions and the thermal and humidity history also significantly affect the samples' tensile strength. This results in different mean tensile strength for samples that were tested on different days [79]. The tensile strength of fibers is affected by various factors, such as atmospheric conditions. Therefore, the nanoparticle-coated sample groups are compared with the bare fiber control group that is prepared on the same day. Figure 3.8 compares 5%, 7.5%, 10%, 12.5%, and 15% ZnO nanoparticle-coated glass fibers and the bare fibers prepared on the same day. Figure 3.9 compares the Weibull plots of these sample groups. Weibull plots slope gives the Weibull modulus of the data groups; an increase in Weibull modulus is desired since it means a decrease in failure probability.

The results of the tensile test show that all the concentrations of ZnO nanoparticle coating improve the tensile strength properties of E-glass fiber. Comparing the Weibull modulus values, all but 15% concentration seem to increase, resulting in an increase in failure probability. Investigating Figure 3.8 and Figure 3.9, information on the effect of nanoparticles on mechanical performance can be obtained.

5ZnCF sample group, compared with it's bare fiber sample group, showed the least improvement compared to the other 4 nanoparticle-coated sample groups. Bare fibers that were prepared on the same day as the 5ZnCF exhibited a tensile strength value of 1384.57 MPa, whereas the 5ZnCF exhibited a tensile strength of 1444.17 MPa, improving the tensile strength by 4.30%. With the increase of nanoparticle concentration to 7.5%, sample group 7.5ZnCF sample group showed a tensile strength of 1531.09 MPa compared to its bare fiber sample group, which has 1394.14 MPa. Increasing the tensile strength performance by 10.62%. The maximum increase in tensile strength was achieved through the 10% ZnO coating with sample group 10ZnCF having a tensile strength of 1490.3 MPa compared to the bare fiber group 1299.68 MPa, increasing the tensile strength of glass fiber up to 14.67%. The increase in tensile strength reaches the saturation point here, decreasing the increase of tensile by further increasing the nanoparticle concentration. 12.5ZnCF sample group also shows improved tensile strength properties compared to the bare fiber sample group. The tensile strength value of the 12.5ZnCF group was calculated to be 1668.62 MPa. Compared to the bare fiber group with a tensile strength of 1516.16 MPa, 7.5% nanoparticle coating exhibited an increase in tensile strength by 11.37%. Finally, the sample group 15ZnCF showed a 7.84% increase in tensile strength.

Table 3.2: Improving effect of different ZnO nanoparticle percentage coatings on Weibull Modulus of E-glass fibers

Sample Type	Bare Fiber	Coated Fiber	Probability of Failure
5ZnCF	2.94	4.29	Lower
7.5ZnCF	3.24	3.32	Lower
10ZnCF	3.39	3.90	Lower
12.5ZnCF	4.60	5.20	Lower
15ZnCF	3.91	3.10	Higher

Table 3.2 compares the final values of the Weibull modulus in different sample groups. Combining the information presented in Figure 3.8, all the different concentrations of ZnO nanoparticle coating show an increase in Weibull modulus with the exception of 15% ZnO coating. Comparing the Weibull modulus of both 5ZnCF and the bare fiber groups, for the bare fiber sample group to have 2.94 and the 5ZnCF group to have 4.29 as the Weibull modulus, the coating increased the Weibull modulus by 45.9%. For the 7.5ZnCF, the increase in Weibull modulus is approximately 3%. As for the 10ZnCF samples, the Weibull modulus was calculated to be 3.90, where the bare fiber was 3.39 resulting in a 15% increase. For the 12.5ZnCF, coated fiber had a Weibull modulus of 5.20 the bare fibers had a Weibull modulus of 4.60, making the increase of Weibull modulus 13%. Finally, the 15ZnCF sample group had a Weibull modulus of 3.10, whereas the bare fiber group had a Weibull modulus of 3.91, resulting in a sharp decrease of 20.5%. This decrease can be attributed to the fact that the high concentration of nanoparticles results in a non-uniform coating generating new stress points, resulting in a higher failure probability [43, 44].

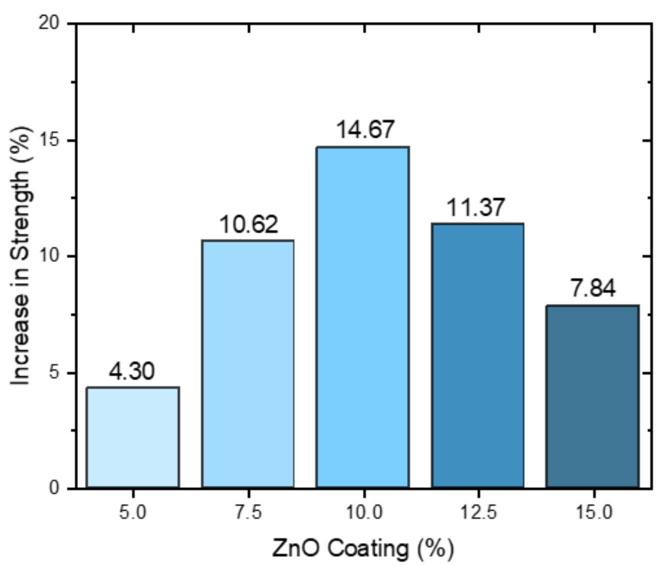

Figure 3.7: Improving effect of different ZnO nanoparticle percentage coatings on tensile strength of E-glass fibers

A comparison of the increase in tensile strength of different nanoparticle concentrations can be seen in Figure 3.7. This figure summarizes and depicts the effect of different ZnO nanoparticles on the tensile strength of E-glass fiber.

Table 3.3: Tensile strength comparison of bare fibers (BF) and coated fibers (CF) for each nanoparticle concentration and increase in tensile strength

	BF Strength (MPa)	CF Strength (MPa)	Increase (%)
5ZnCF	1384.57	1444.17	4.30
7.5ZnCF	1384.14	1531.09	10.62
10ZnCF	1299.68	1490.30	14.67
12.5ZnCF	1516.16	1688.62	11.37
15ZnCF	1390.18	1499.23	7.84

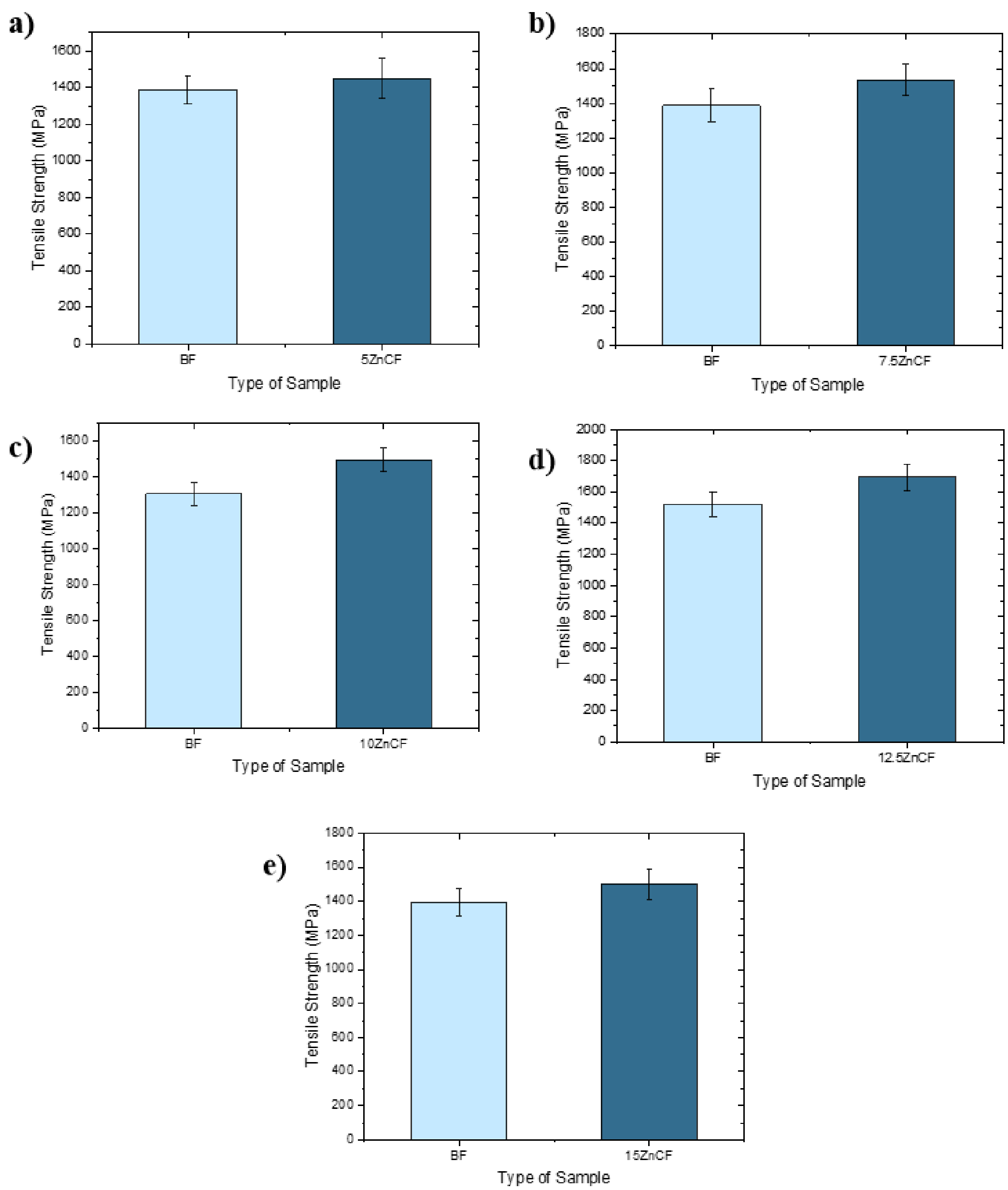

Figure 3.8: Improving effect of different ZnO nanoparticle percentage coatings on tensile strength of E-glass fibers

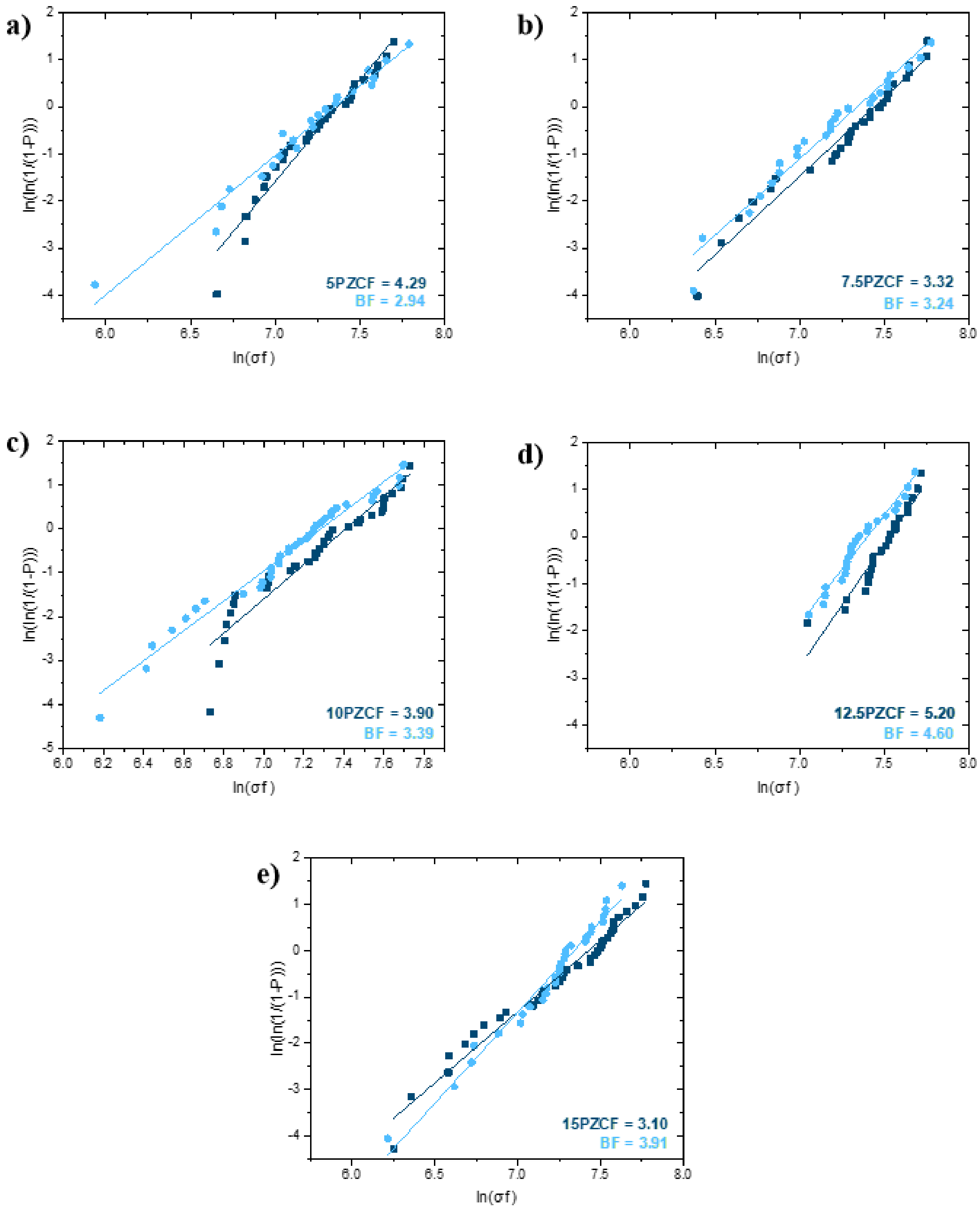

Figure 3.9: Improving effect of different ZnO nanoparticle percentage coatings on Weibull plots

3.2.6 Acid Solution Performance

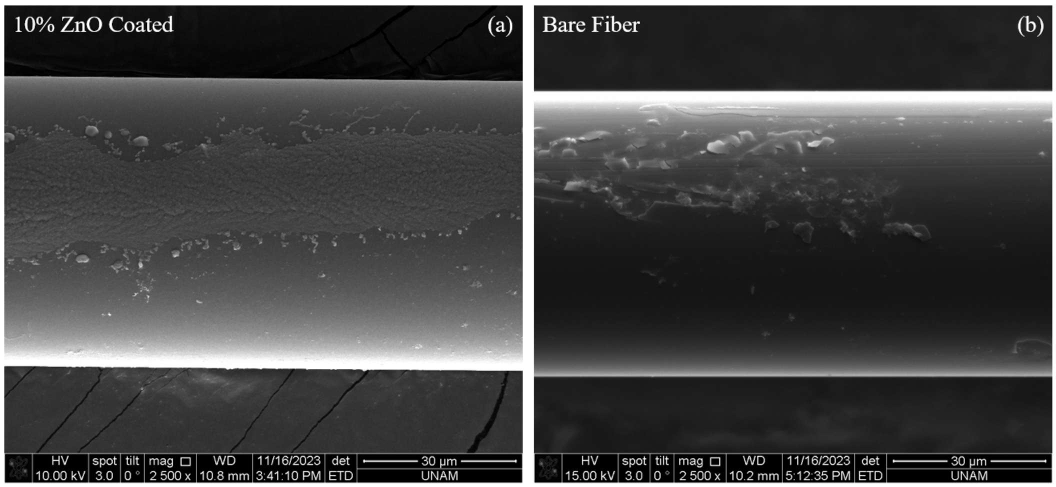

Figure 3.10: SEM images of a) 10% ZnO nanoparticle coated and b) bare fiber after 24 hours of acidic environment exposure

For the acid test, the bare fibers and the 10% ZnO coated fibers are exposed to an acidic 37% HCl solution for 24 hours to investigate the effect of ZnO nanoparticles on the acid resistance of fibers. The experiment was conducted in the cleanroom with a fume hood. Only 10% solution is used since they exhibit the best mechanical performance. After the acid test, the fibers are rinsed with DI water to remove any residual HCl on the surface. The acidic corrosion on the glass fiber surface is due to the ion exchange between the metal ions present on the glass surface, such as calcium and alumina, and the hydrogen ion from the acidic environment [80]. In order to prevent HCl from attacking the glass surface, ZnO nanoparticle coating is used to minimize the damage by acting as a protective layer on the glass surface. Figure 3.10 shows the comparison of the sample surfaces after 24 hours of acid exposure. 10% nanoparticle coating visibly has a residue from the ZnO coating and no visible damage to the actual glass surface. Compared to the bare fiber with visible surface damage caused by the acidic environment.

3.2.7 Electromagnetic Performance

Depending on the application, it is desired for glass fiber composites to have good RF transmittance. The introduction of metal oxide nanoparticles such as ZnO onto the glass fiber will alter the overall electromagnetic properties of the glass fiber resin composite. Network analysis is conducted on the prepared glass fiber felt composites to determine the effect of nanoparticles. The measurements were taken using Keysight Network Analyzer E5063A. The felt fiber composites are placed inside the sample compartment of the network analyzer. The samples are subjected to X-Band frequencies (8.2 - 12.4 GHz). Previously, the addition of metal oxide nanoparticles increased the conductivity and shielding effect of the materials embedded in [81, 82, 83]. The results show that the addition of nanoparticles increases the overall dielectric constant of the composite material. This caused a 3.29% increase in the reflective properties of the composite material.

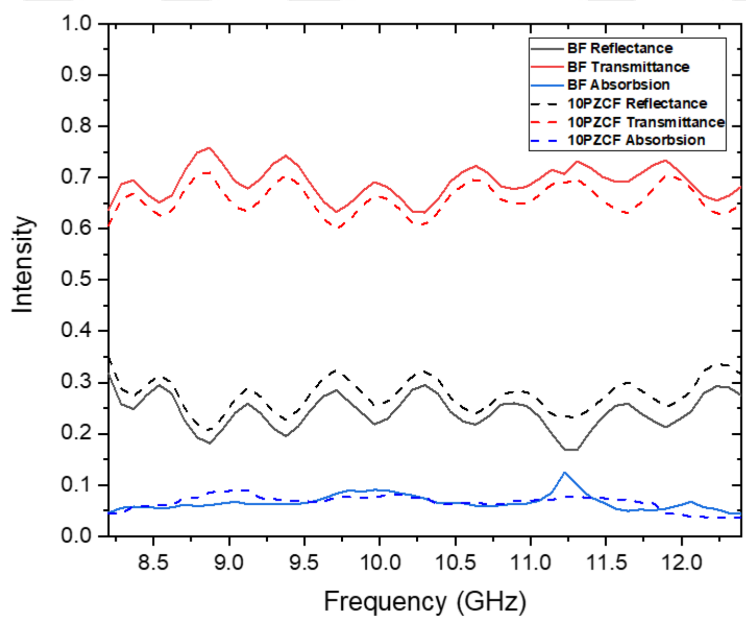

Figure 3.11: Network Analyzer results of BF felt composite and 10ZnCF felt composite

3.3 Conclusion

This chapter investigated the effect of ZnO nanoparticle coating on the mechanical and chemical properties of the E-glass fiber. This investigation includes the morphological, spectroscopic, fractographic, chemical, and statistical mechanical properties. Morphological and spectroscopic analyses confirmed that the surface of glass fibers was coated with ZnO nanoparticles. For all the different ZnO nanoparticle concentration solutions, the tensile strength value of the glass fibers increased. As for the Weibull modulus, all but the 15% solution proved to decrease the failure probability. An increase in 15% solution failure probability can be attributed to the flaws induced by the high concentration of the ZnO nanoparticles. The overall best increase in tensile strength was achieved by 14.67% with 10% ZnO nanoparticle coating. Figure 3.9 shows that the increase in tensile strength reaches saturation at the 10% nanoparticle concentration mark and starts to decrease with the further increment of the solution concentration. Acid test showed that the ZnO nanoparticle coating provide chemical resistance to the glass fibers in acidic environments. A further investigation showed ZnO coating cause a slight 3.29% increase in the reflective properties of glass fiber composite.

Chapter 4

Fabrication of Pure Silica Fiber

4.1 Introduction

Reinforcement fibers are added to the resin matrix for various reasons. With the addition of reinforcement fibers, the primary effect is the increase in the mechanical performance of the epoxy/resin matrix. Properties such as thermal expansion and dielectric properties are also considered for various specialized applications. A common glass fiber composite uses E-glass fiber for the reinforcement components. E-glass has approximately 52 to 56% Silica in its composition. Other materials present in the glass composition alter the dielectric properties in a negative way, reducing the signal transmittance of the composite material. High signal transmittance property is important in applications such as communication and radar. Radomes (radar domes) of planes are constructed from glass fiber composites [6]. The metal oxides and minerals present in the E-glass increase the overall dielectric constant of the composite material, reducing the transmittance and creating noise in signal [84]. As an alternative reinforcement, pure silica fiber is considered a perfect alternative [85]. Having no metal oxides in its composition silica fiber composites provide the desired signal transmission for RF communications [61].

Pure silica fibers or fused silica fibers are glass fibers that contain 99.95% silica in their chemical composition. It is also known as quartz fiber in the composite industry. Even though it is called quartz, the silica fiber used for composite applications is indeed amorphous. Silica fibers have desirable properties such as a small thermal expansion coefficient, thermal insulation, and excellent dielectric properties [84]. Silica fibers have almost purely silica in their chemical composition. This results in an extremely low dielectric constant, making the silica fiber-reinforced composites a perfect candidate for specialized use in aerospace applications. Silica fibers are currently commercially available in fabric both woven and unwoven forms [84, 86].

4.2 Fabrication of Pure Silica Fiber

Fabrication of pure silica fiber is similar to fabricating any other fiber. In order to form silica material into a fiber form, the silica rod is heated above its glass transition temperature. The glass transition and melting temperature of pure silica, when compared to the E-glass, is higher. The softening point for a commercially available E-glass fiber is 840°C, whereas the softening temperature for pure silica is 1675°C [87]. This requires a different setup to heat the raw materials beyond the softening temperature. Construction of a conventional continuous glass fiber production setup is not an option due to its production scale and cost. Therefore, a relatively simple and cost-effective method was needed to fabricate pure silica fiber. As seen in Figure 4.1, one method to fabricate fiber is to single-fiber fabrication method for optical glass fibers. This is a more precise method that is used to fabricate single fibers that are used in various applications such as communication, lasers and sensors. A generic single fiber drawing setup is composed of a draw tower which includes a resistance or induction furnace, a specialized chuck to hold the fiber preform, capstan tractor, sizing applicator, and a winding equipment [88].

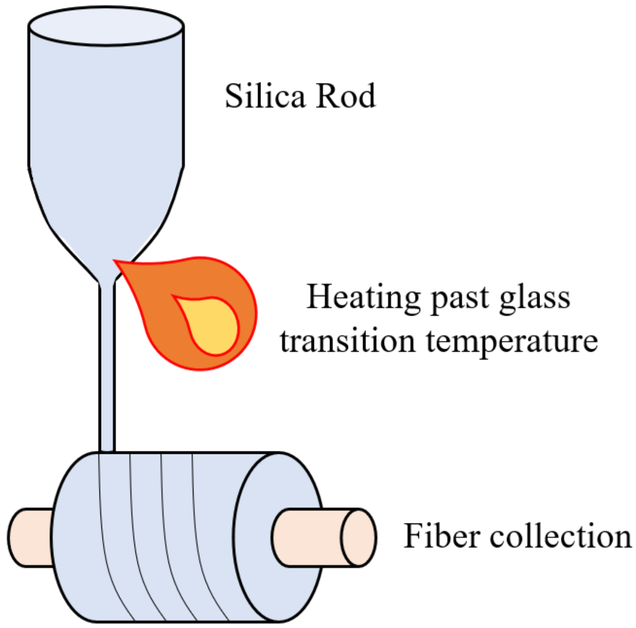

Figure 4.1: Schematic illustration of single fiber drawing process.

4.2.1 Methodology

The fabrication of pure silica fiber starts with the construction of a drawing setup. The production approach taken to produce the single silica fiber is similar to the optical fiber drawing method. In the common optical fiber drawing setups, the heat source is an induction furnace. In this study, the source of heating is preferred to be an oxy-fuel gas system to reduce the construction costs of the setup. There are two options commercially available that can reach the desired temperatures. These options are oxy-acetylene and oxy-hydrogen setups. The material that is used for this study is pure silica rods with 10 mm and 6mm diameters supplied from SA-HA Labware Ltd., Ankara.

4.2.2 Design of Fiber Drawing Setup

Construction of the drawing setup started with the construction of the frame of the structure. The frame is constructed from aluminum sigma profiles. This

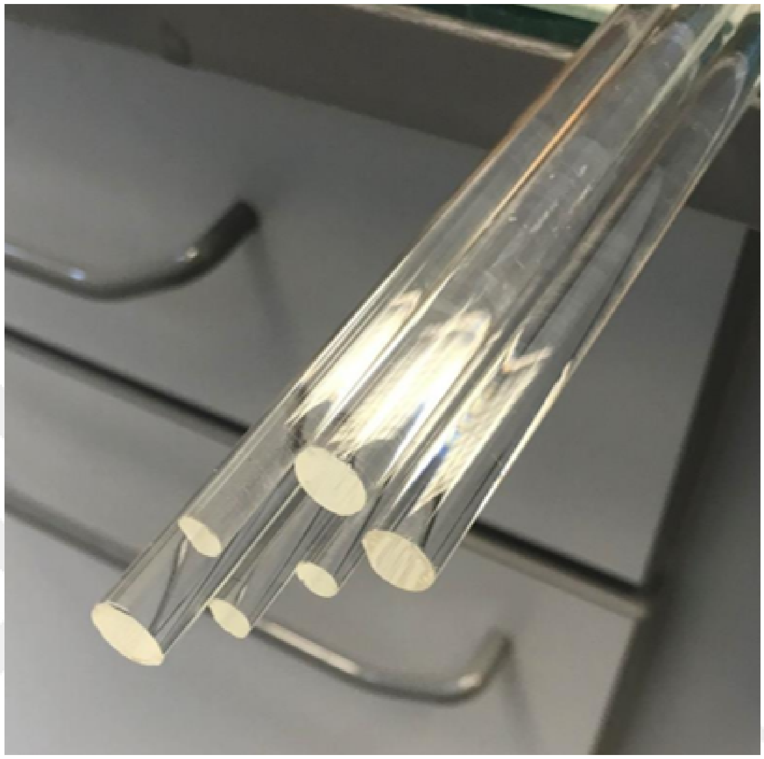

Figure 4.2: Image of pure silica rods.

was preferred because of its easy construction and high thermal conductivity. The outer and inner walls of the drawing setup are made from a ceramic wool insulation material sandwiched between two sheet metals. A borosilicate glass window is added to the door of the setup to monitor the process. The setup is designed to have multiple functioning components such as a gas system, temperature measurement system, ventilation system, capstan tractor, and feeding mechanism.

The fiber drawing setup is designed to reach temperatures above 1600 °C. The setup needed to be designed according to the safety regulations since these types of gas systems are dangerous. The gas system is preferred to be an oxygen-hydrogen fuel gas system. The reason behind this choice was the oxy-acetylene setup produced gasses such as carbon monoxide that create undesired carbon pollution. In addition to the pollution, the flame produced by this system proved to be unstable and caused harm to the silica fiber when the diameter decreased. Compared to the oxy-acetylene system, the oxy-hydrogen system produced a

Figure 4.3: Rendered image of fiber drawing setup and photograph of the constructed drawing setup.

stable and clean flame that is able to heat the silica rod past its glass transition temperature. Installation of the gas system required multiple levels of safety precautions. The requirements state that the oxygen and fuel tanks need to be separate and outside the building. This required the installation of a gas line infrastructure to transport the gasses from the outside into the laboratory.

Gas system has several safety precautions places such as double check valves on both oxygen and hydrogen gas lines. Manual hand valves to cut the gas lines. A vent hood is also constructed to evacuate any residual gasses from the burning chamber and laboratory. The ventilation system consists of a sheet metal fume hood that is directly connected to the burning chamber. The fume hood is connected to a fan motor that sucks the gasses from the drawing system. The setup included a commercial-use oxy-fuel gas torch head. Single nozzle torch with 2 precise valves to control the flow of the oxygen and fuel gas. This is replaced with a custom-designed 4-nozzle torch. Providing more uniform heating for silica rods to exceed the glass transition temperature. The nozzle features a 25° upward angle to prevent the oxy-hydrogen flame from heating the copper alloy torch.

The temperature of the process is monitored using a FLUKE Thermoalert 3.0

Pyrometer. The pyrometer is installed aimed at the silica rod's necking region to monitor the temperature of the process. The outer layer of the pyrometer is connected to a thermal cooling jacket with an atmospheric air cooling system. Being inside the drawing system, cooling is necessary to protect equipment from temperature-related damages. The pyrometer is connected to a computer for reading accurate temperature data.

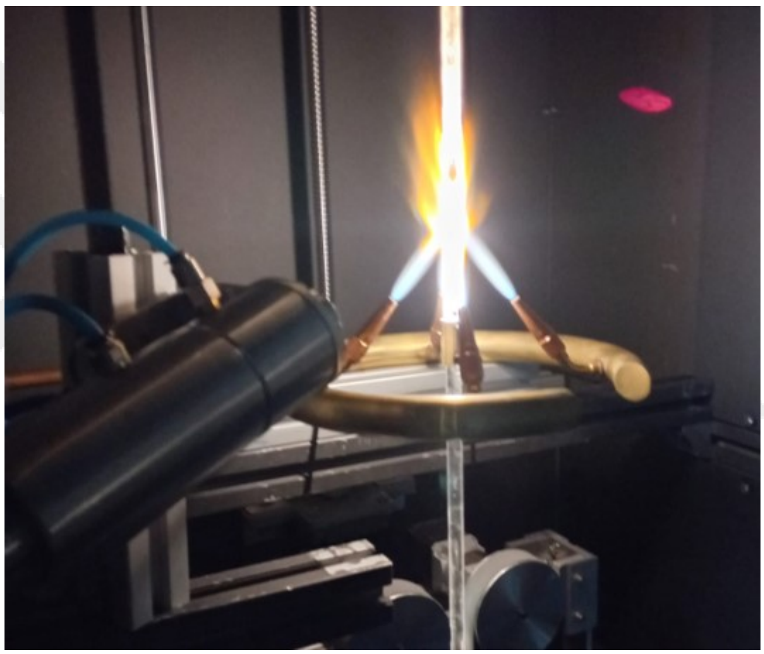

Figure 4.4: Image of pyrometer measuring the temperature of the necking process.

The fiber diameter is controlled by a device called a capstan tractor. For convenience, further mentions will be referred to as capstan. A capstan is a machine that pulls the fiber down in a linear manner and determines the final diameter of the fiber. Figure 4.5 shows the rendering of the capstan machine designed using SolidWorks CAD software.

The upper pulleys that are seen on the rendering are connected to gearboxes that provide the required torque for pulleys to turn with enough speed. Gearboxes are attached to two stepper motors that power the pulley system. Motors are connected to a setter motor driver that is connected to an Arduino Mega board. Another stepper motor controls the distance between the pulleys and provides symmetrical movement, keeping the fiber centered. This movement is obtained

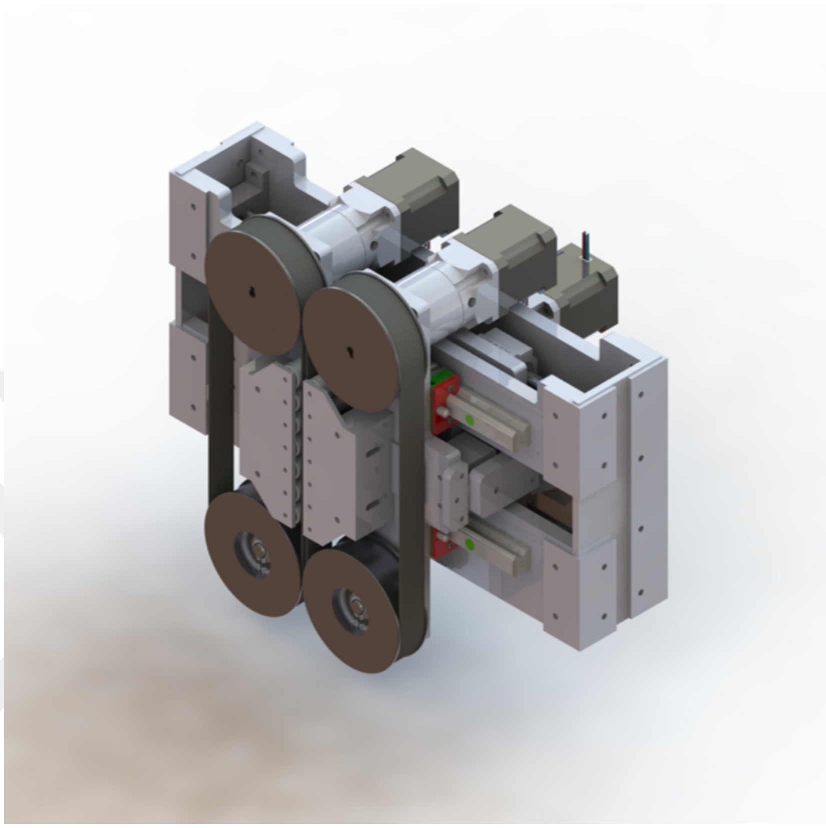

Figure 4.5: Rendered image of capstan machine.

by utilizing a pinion rack system that is directly attached to the platform that has two symmetrical pulleys and conveyor belts. Conveyor belts provide the required support for rubber bands to create enough friction force to pull the fiber. The conveyor belt system includes a suspension system on both sides of the capstan to tolerate sudden changes in the glass fiber diameter. Pulling speed is controlled and monitored using a custom-built control box and an LCD screen. The main body of the capstan machine is constructed from 6000-grade aluminum to reduce weight and to have greater thermal cooling properties.

The feeder mechanism, as the name suggests, feeds the system with the silica rod. The basic structure is composed of 2 moving platforms, allowing 2-dimensional movement for the attached silica rod. This mechanism allows the silica rod to be centered in the heating zone. It is planned to be fully computer-controlled and automated, but currently, centering is manually done. The most

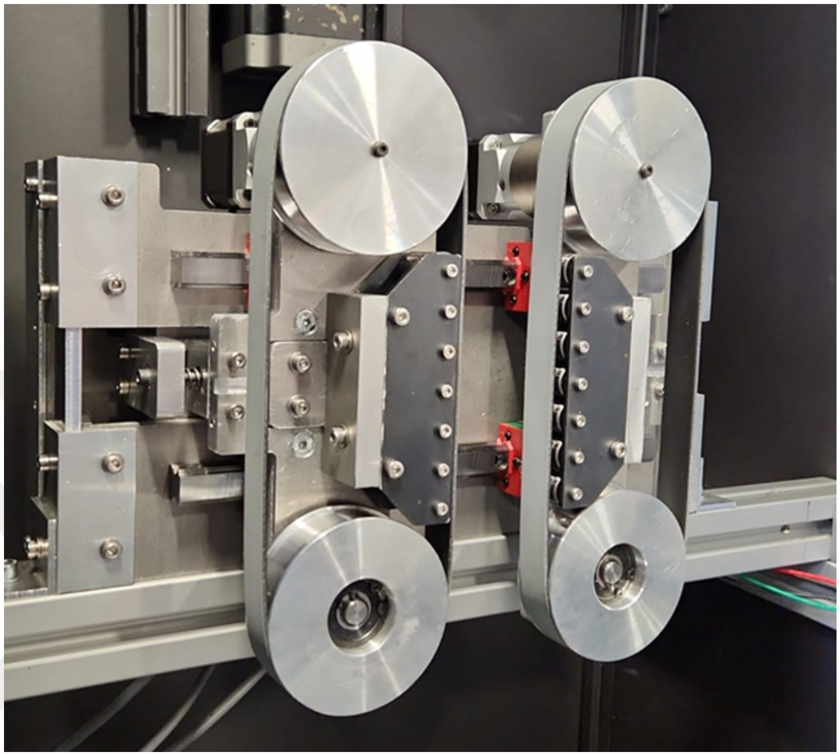

Figure 4.6: Photograph of the manufactured capstan machine.

important feature of the feeder mechanism is its vertical movement. The vertical movement speed is controlled via computer. A stepper motor is connected to a threaded shaft to convert the rotational movement into linear movement. The structure is supported by two linear 16 mm diameter shafts, and 4 sets of linear bearings provide stable vertical movement. The silica rod is attached to a steel drill chuck. To prevent fracture due to the contact surface between steel and silica, the ends of the silica rods are covered with Teflon band. The band also provides friction to hold the silica rod.

4.3 Results

The custom-built oxy-hydrogen heating system provided the required heat to heat the silica rod samples above the glass transition temperature to draw them into fibers. 5 meters of continuous fiber fabrication was successfully drawn with

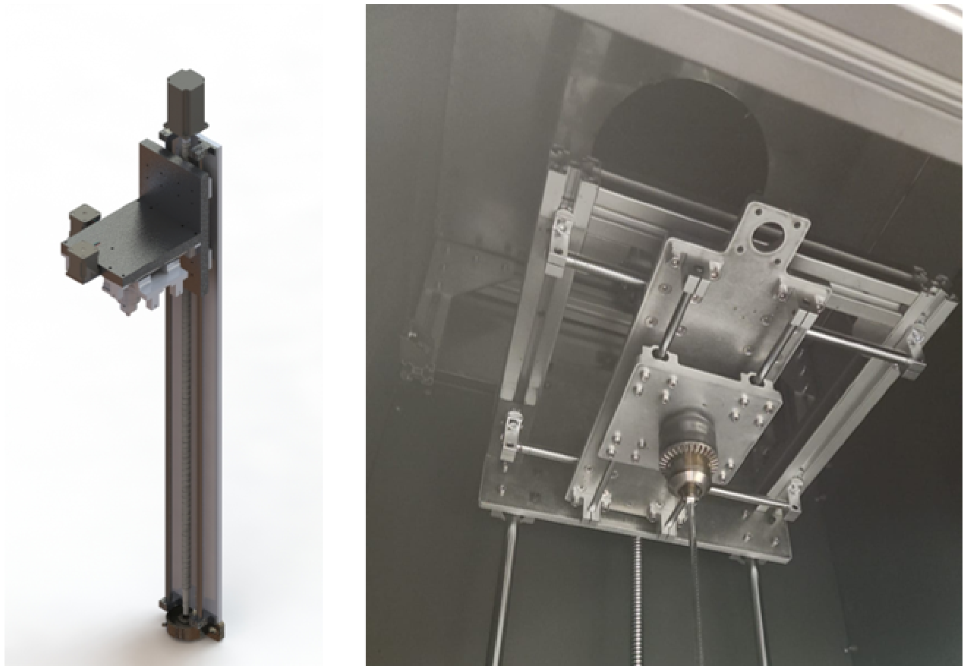

Figure 4.7: Rendered design and the photograph of feeder mechanism.

the current heating system. The fabricated single fiber samples are characterized under the Keyence VKX 100 Microscope and ZEISS AX10 Optical Microscope to evaluate the dimensions. Figure 4.8 shows the microscope images of the manufactured fibers. Fibers fabricated proved to have a non-uniform diameter throughout their length. This may be due to the 4 nozzle heating system. In order to increase the uniformity of heating, a new heating system is required. The design of the new heating system is started, and drawing fiber with a uniform diameter under 50 μm is planned.

4.4 Conclusion

A novel method for drawing pure silica fibers from a silica rod is established. Compared to the alternative fiber fabrication methods, compact and cost-effective fiber drawing setup is constructed. Using the drawing setup a pure silica fiber with non-uniform diameter under 100 μm is fabricated and collected. Current

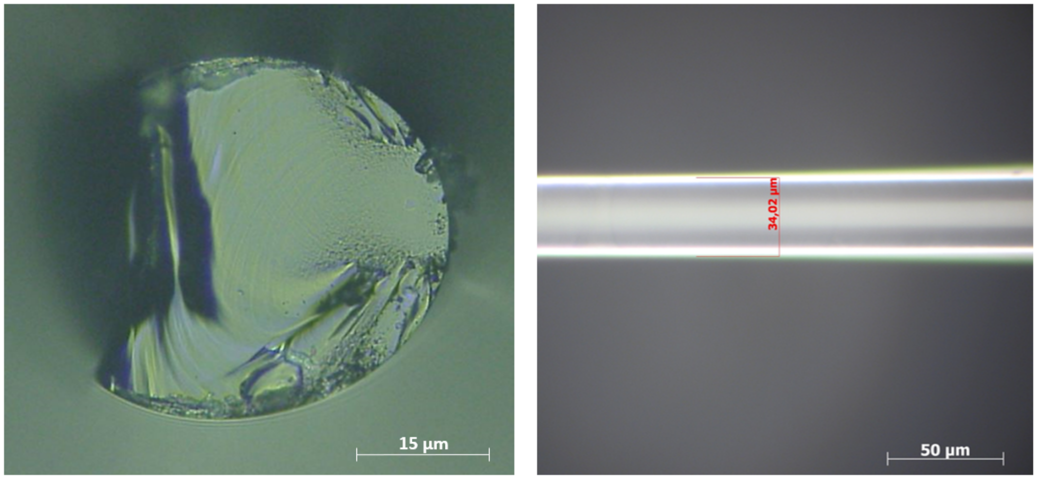

Figure 4.8: Cross-sectional image and the diameter measurement of the fabricated silica fiber.

custom torch nozzle causes unstable flame causing the changes in the diameter. A new heating system is required to be manufactured in order to achieve better control over the flames and achieve homogeneous heating.

Chapter 5

Conclusion and Future Works

Glass fibers are the most preferred option in the fiber-reinforced resin matrix composite field, Dominating the market share by 95%. In glass fibers, the market is dominated by E-glass fibers, making 90% of the market [6]. This research on glass fibers aims to improve the mechanical and chemical performances of glass fibers using a relatively straightforward method. By improving the performance of the glass fibers, overall composite performance can also be improved significantly. This thesis investigates the effect of ZnO nanoparticle coatings on the mechanical and chemical properties of E-glass fibers. Focusing on the performance of single glass fibers makes a relatively fundamental approach to one of the key components of glass fiber-reinforced composites. In previous work, different types of nanoparticles, such as TiO_2, SiO_2, and ZrO_2, were investigated, and this thesis investigates the different concentrations (5%, 7.5%, 10%, 12.5%, and 15%) of ZnO nanoparticles. By dip-coating the E-glass fibers in DI water and nanoparticle solutions, the properties such as the tensile strength of coated and bare fibers are investigated. A sizing agent (1% APTES) is also applied on the glass fiber surface using dip-coating. The fibers that were prepared were characterized using SEM, XPS, EDX, and XRD. The samples underwent micromechanical tests to investigate the mechanical properties of glass fibers and the effect of ZnO nanoparticles on the tensile strength of glass fibers. Characterizations confirmed that the ZnO water dispersion solutions were indeed ZnO, and the solutions were stable. Micromechanical tests concluded that the optimum nanoparticle concentration for this test was 10% ZnO, providing a 14.67% increase in the tensile strength and a 15% decrease in the failure probability of glass fibers. The correlation between the size of the mirror region and the tensile strength of the fiber was also confirmed. The acid test result proved that the ZnO coating protects the glass fibers from an acidic environment (37% HCl) for 24 hours. Using the Nicholson Ross Weir (NWR) method, the transmission, absorption, and reflection values of the glass fiber felt composites were measured. The addition of ZnO nanoparticles on the glass fiber surface increased the reflection values of composite material by 3.29%.

As for the production of the silica fiber section, a different approach to produce the silica fiber was taken. A new setup was manufactured to draw the silica fiber from silica rods with 6 and 10-mm diameters. The fiber drawing started with a single nozzle torch. Unidirectional flame resulted in uneven necking. This is due to flame being sent out from a single nozzle. To solve the problem, a custom torch head with 4 nozzles is manufactured. Nozzles had equal spacing between them. Using this setup, a relatively uniform heating was achieved, and the first fibers were drawn. However, due to the difference in pipe length between each other, the flow of the fuel gasses was not stable. A silica fiber with nonuniform diameters under 100 μm was successfully drawn.

Future work for this study is to investigate the effect of nanoparticle size on the mechanical and chemical properties of the glass fibers. The size of ZnO nanoparticles used in this study was between 25 to 35 nm. The effect of size on the quality and uniformity of the coating is planned to be investigated. In this study, glass fiber composites used to investigate the effect of nanoparticles on the electromagnetic properties are prepared as glass fiber felt composites. Since the investigation is only focused on the electromagnetic properties, the composite materials were designed as felt reinforcement. In the future, the aim is to fabricate a nanoparticle-coated glass fiber fabric composite. Since the nanoparticle coating improved the mechanical and chemical properties of the glass fibers, it is expected also to improve the glass fiber composites. The effect of nanoparticles on the performance of the fiber-matrix interface and the effect on the mechanical properties of composite is planned to be investigated.

For the fabrication of the silica fiber, the heating system will manufactured as a custom design to achieve a more homogeneous and stable source of heating. The current heating system is heavily dependent on the skill of the operator. It is planned to be replaced with micrometer-accurate valves to reduce the operator skill dependency and have precise control over the flow of the gasses. Depending on the design of the heating system, additional thermal supporting systems such as a cooling system and insulation may be required. The control mechanism of the feeder system is currently semi-automatic. While the feeding action is fully computer-controlled, the centering of the silica rods is manually achieved. This limits the intervention capabilities while a fiber drawing is in process. In the future, with the addition of extra stepper motors, the horizontal movement of the feeder will be fully automated and controlled with a computer. A continuous silica fiber fabrication of 50 meters is planned. All the systems are planned to connect to a single computer and controlled.

Bibliography

[1] W. Commons, "B735 wetter radar," 2008.

[2] R. Limited, "Fibreglass cloth, mat and tape for all your composite needs in canada."

[3] E. Martynova and H. Cebulla, "Chapter 7 - glass fibers," in *Inorganic and Composite Fibers* (B. Mahltig and Y. Kyosev, eds.), The Textile Institute Book Series, pp. 131–163, Woodhead Publishing, 2018.

[4] F. T. Wallenberger and P. A. Bingham, "Fiberglass and glass technology," *Energy-Friendly Compositions And Applications*, 2010.

[5] K. L. Loewenstein, "The manufacturing technology of continuous glass fibres," 1973.

[6] A. Cevahir, "Glass fibers," in *Fiber Technology for Fiber-Reinforced Composites*, pp. 99–121, Elsevier, 2017.

[7] J. P. Srivastava and P. Kumar, *Introduction to Glass Fiber-Based Composites and Structures*, ch. 1, pp. 1–16. John Wiley and Sons, Ltd, 2022.

[8] S. G., "Method and apparatus for making glass wool," May 3 1938. U.S. Patent 2133 235.

[9] F. Aramide, P. Atanda, and O. Olorunniwo, "Mechanical properties of a polyester fibre glass composite," *International Journal of Composite Materials*, vol. 2, no. 6, pp. 147–151, 2012.

[10] H. Li, T. Charpentier, J. Du, and S. Vennam, "Composite reinforcement: Recent development of continuous glass fibers," *International Journal of Applied Glass Science*, vol. 8, no. 1, pp. 23–36, 2017.

[11] H. Li, P. Gu, J. Watson, and J. Meng, "Acid corrosion resistance and mechanism of e-glass fibers: boron factor," *Journal of Materials Science*, vol. 48, pp. 3075–3087, 2013.

[12] J. Thomason, "Interfaces and interfacial effects in glass reinforced thermoplastics-keynote presentation," 2007.

[13] J. W. Hearle, *High-performance fibres.* Elsevier, 2001.

[14] M. O. Seydibeyoglu, A. K. Mohanty, and M. Misra, *Fiber technology for fiber-reinforced composites.* Woodhead Publishing, 2017.

[15] Z.-M. Huang, "Biocomposites," in *Comprehensive Structural Integrity (Second Edition)* (M. H. F. Aliabadi and W. O. Soboyejo, eds.), pp. 197–263, Oxford: Elsevier, second edition ed., 2023.

[16] B. Mahltig and Y. Kyosev, "Inorganic and composite fibers: production, properties, and applications," 2018.

[17] J. M. Stickel and M. Nagarajan, "Glass fiber-reinforced composites: from formulation to application," *International Journal of Applied Glass Science*, vol. 3, no. 2, pp. 122–136, 2012.

[18] B. Mrduljaš, A. Baričević, I. Pucić, I. Carević, and K. Didulica, "Alkali resistance of selected waste fibres to model cement environment," *Case Studies in Construction Materials*, vol. 19, p. e02411, 2023.

[19] A. Nourredine, L. Molez, and D. Rangeard, "Durability of alkali-resistant glass fibers reinforced cement composite: Microstructural observations of degradation," *Periodica Polytechnica Civil Engineering*, vol. 62, 02 2018.

[20] R. Karell, J. Kraxner, M. Chromcikova, and M. Liska, "Properties of selected zirconia containing silicate glasses iii," *Ceramics - Silikaty*, vol. 51, pp. 125–130, 01 2007.

[21] S. Gao, E. Mäder, A. Abdkader, and P. Offermann, "Environmental resistance and mechanical performance of alkali-resistant glass fibers with surface sizings," *Journal of Non-Crystalline Solids*, vol. 325, pp. 230–241, 09 2003.

[22] E. Mäder, R. Plonka, M. Schiekel, and R. Hempel, "Coatings on alkali-resistant glass fibres for the improvement of concrete," *Journal of Industrial Textiles - J IND TEXT*, vol. 33, pp. 191–207, 01 2004.

[23] T. Sathishkumar, S. Satheeshkumar, and J. Naveen, "Glass fiber-reinforced polymer composites – a review," *Journal of Reinforced Plastics and Composites*, vol. 33, no. 13, pp. 1258–1275, 2014.

[24] H. Liu, Y. Yu, Y. Liu, M. Zhang, L. Li, L. Ma, Y. Sun, and W. Wang, "A review on basalt fiber composites and their applications in clean energy sector and power grids," *Polymers*, vol. 14, p. 2376, June 2022.

[25] S. Yasufuku, "Application of glass fiber-reinforced plastics to electrical and electronic apparatus in japan," *IEEE Electrical Insulation Magazine*, vol. 10, no. 1, pp. 8–15, 1994.

[26] G. Yang, M. Park, and S.-J. Park, "Recent progresses of fabrication and characterization of fibers-reinforced composites: A review," *Composites Communications*, vol. 14, 05 2019.

[27] I. Al-Janabi, S. A. Odaa, K. Hasan, and M. A. Al-Kubaisi, "Properties evaluation of fiber reinforced polymers and their constituent materials used in structures – a review," *Materials Today: Proceedings*, vol. 43, pp. 1003–1008, 04 2021.

[28] K. Chawla, "Glass fibers," *Encyclopedia of Materials: Science and Technology*, 12 2016.

[29] F. Wallenberger and P. Bingham, *Fiberglass and Glass Technology*. 01 2010.

[30] H. Li, P. Gu, J. Watson, and J. Meng, "Acid corrosion resistance and mechanism of e-glass fibers: Boron factor," *Journal of Materials Science*, vol. 48, no. 8, p. 3075–3087, 2013.

[31] P. Cousin, M. Hassan, P. Vijay, M. Robert, and B. Benmokrane, "Chemical resistance of carbon, basalt, and glass fibers used in frp reinforcing bars," *Journal of Composite Materials*, vol. 53, p. 002199831984430, 04 2019.

[32] M. Y. Khalid, Z. U. Arif, W. Ahmed, and H. Arshad, "Evaluation of tensile properties of fiber metal laminates under different strain rates," *Proceedings of the Institution of Mechanical Engineers, Part E: Journal of Process Mechanical Engineering*, vol. 236, no. 2, pp. 556–564, 2022.

[33] M. Y. Khalid, A. A. Rashid, Z. U. Arif, N. Akram, H. Arshad, and F. P. García Márquez, "Characterization of failure strain in fiber reinforced composites: Under on-axis and off-axis loading," *Crystals*, vol. 11, p. 216, Feb. 2021.

[34] A. V P, K. Arumugam, and K. Muthusamy, "Evaluation of mechanical properties of banana and sisal fiber reinforced epoxy composites: Influence of glass fiber hybridization," *Materials Design*, vol. 64, p. 194–202, 12 2014.

[35] H. R. Phlllpp, "Silicon Dioxide (SiO ,) (Glass)," *Handbook of Optical Constants of Solids - Vol 1, Part 2, subpart 3*, pp. 749–763, 1985.

[36] X. Han, "Investigation on the complex interaction between particle and substrate in mechanical polishing of silica glass," *International Journal of Advanced Manufacturing Technology*, vol. 85, no. 9-12, pp. 2567–2575, 2016.

[37] F. T. Wallenberger, "Structural Silicate and Silica Glass Fibers," no. Figure 1, pp. 129–168, 2000.

[38] T. Miyashita and T. Manabe, "Infrared Optical Fibers," *IEEE Transactions on Microwave Theory and Techniques*, vol. 30, no. 10, pp. 1420–1438, 1982.

[39] N. Chillu, A. Jeshurun, R. Jayaganthan, R. Velmurugan, and R. Sarathi, "Investigation on dielectric and mechanical properties of epoxy reinforced with glass fiber and nano-silica composites," *Materials Research Express*, vol. 6, no. 11, 2019.

[40] R. Brückner, "Properties and structure of vitreous silica. I," *Journal of Non-Crystalline Solids*, vol. 5, no. 2, pp. 123–175, 1970.

[41] J. L. Thomason, "Glass fibre sizing: A review," *Composites Part A: Applied Science and Manufacturing*, vol. 127, p. 105619, 2019.

[42] E. P. Plueddemann, *Nature of adhesion through silane coupling agents*. Springer, 1991.

[43] M. K. Ahmed, A. B. Behboud, A. Kurucu, G. K. Çömlekçi, and M. Ordu, "Improved mechanical properties of the E-glass fibres through TiO_2 nanoparticle coating," *Materials Science and Technology*, vol. 39, no. 11, pp. 1304–1312, 2023.

[44] A. B. Behboud, M. K. Ahmed, A. Kurucu, G. K. Çömlekçi, and M. Ordu, "Zirconia nanoparticle coating for high-strength and alkali-resistant glass fibers," *Journal of Non-Crystalline Solids*, vol. 619, p. 122571, 2023.

[45] P. Zinck, E. Mäder, and J.-F. Gerard, "Role of silane coupling agent and polymeric film former for tailoring glass fiber sizings from tensile strength measurements," *Journal of materials science*, vol. 36, pp. 5245–5252, 2001.

[46] J. Karger-Kocsis, H. Mahmood, and A. Pegoretti, "Recent advances in fiber/matrix interphase engineering for polymer composites," *Progress in Materials Science*, vol. 73, pp. 1–43, 2015.

[47] Q. An, S. Tamrakar, J. W. Gillespie Jr, A. N. Rider, and E. T. Thostenson, "Tailored glass fiber interphases via electrophoretic deposition of carbon nanotubes: Fiber and interphase characterization," *Composites Science and Technology*, vol. 166, pp. 131–139, 2018.

[48] C. Scheffler, S. Gao, R. Plonka, E. Mäder, S. Hempel, M. Butler, and V. Mechtcherine, "Interphase modification of alkali-resistant glass fibres and carbon fibres for textile reinforced concrete i: Fibre properties and durability," *Composites Science and Technology*, vol. 69, no. 3-4, pp. 531–538, 2009.

[49] Y. Dong, Y. Zhu, Y. Zhao, F. Liu, E. Wang, and Y. Fu, "Enhance interfacial properties of glass fiber/epoxy composites with environment-friendly water-based hybrid sizing agent," *Composites Part A: Applied Science and Manufacturing*, vol. 102, pp. 357–367, 2017.

[50] Q. An and N. Andrew, “Hierarchical composite structures prepared by electrophoretic deposition of carbon nanotubes onto glass fibers,” *ACS applied materials & interfaces*, vol. 5, pp. 2022–2032, 2013.

[51] Q. An, A. N. Rider, and E. T. Thostenson, “Electrophoretic deposition of carbon nanotubes onto carbon-fiber fabric for production of carbon/epoxy composites with improved mechanical properties,” *Carbon*, vol. 50, no. 11, pp. 4130–4143, 2012.

[52] D. B. Dingwell, “Redox viscometry of some fe-bearing silicate melts,” *American Mineralogist*, vol. 76, no. 9-10, pp. 1560–1562, 1991.

[53] B. O. Mysen, “Redox equilibria and coordination of fe2+ and fe3+ in silicate glasses from 57fe mossbauer spectroscopy,” *Journal of Non-Crystalline Solids*, vol. 95, pp. 247–254, 1987.

[54] C. L. McKinnis, “E-glass batch melting redox and its effect on specific glass properties,” *Journal of Non-Crystalline Solids*, vol. 84, no. 1-3, pp. 381–389, 1986.

[55] M. D. Lund and Y. Yue, “Impact of drawing stress on the tensile strength of oxide glass fibers,” *Journal of the American Ceramic Society*, vol. 93, no. 10, pp. 3236–3243, 2010.

[56] S. Gunal, E. Sayar, B. Geygel, S. Hacıoğulları, N. Karaca, M. Uçar, E. Selver, N. Solak, M. Baydogan, H. Önen, and N. Ucar, “Thermal insulation properties of glass fiber epoxy composite with stonewool fiber, nanofiber web, silica aerogel layers,” 01 2020.

[57] A. Majumdar and R. Nurse, “Glass fibre reinforced cement,” *Materials Science and Engineering*, vol. 15, no. 2, pp. 107–127, 1974.

[58] J. Ahmad, R. A. González-Lezcano, A. Majdi, N. Ben Kahla, A. F. Deifalla, and M. A. El-Shorbagy, “Glass fibers reinforced concrete: Overview on mechanical, durability and microstructure analysis,” *Materials*, vol. 15, no. 15, p. 5111, 2022.

[59] M. A. Faizal, Y. K. Beng, and M. N. Dalimin, "Tensile property of hand lay-up plain-weave woven e-glass/polyester composite: Curing pressure and ply arrangement effect," *Journal of Science and Technology*, vol. 19, 2006.

[60] L. W. H. Leonard, K. J. Wong, K. O. Low, and B. F. Yousif, "Fracture behaviour of glass fibre-reinforced polyester composite," *Proceedings of the Institution of Mechanical Engineers, Part L: Journal of Materials: Design and Applications*, vol. 223, no. 2, pp. 83–89, 2009.

[61] C. Dong, J. Jianguo, and H. Xufeng, "Dielectric properties of quartz fiber reinforced kh308 composites," *Acta Materiae Compositae Sinica*, vol. 31, no. 3, pp. 563–568, 2014.

[62] S. Rehnmark, "On the calibration process of automatic network analyzer systems (short papers)," *IEEE Transactions on Microwave Theory and Techniques*, vol. 22, no. 4, pp. 457–458, 1974.

[63] M. L. Korwin-Edson, D. A. Hofmann, and P. B. McGinnis, "Strength of high performance glass reinforcement fiber," *International journal of applied glass science*, vol. 3, no. 2, pp. 107–121, 2012.

[64] M. Lund and Y. Yue, *Tensile strength of glass fibers.* Faculty of Engineering and Science, Aalborg University, 2010.

[65] S. Freiman, "The fracture of glass: past, present, and future," *International Journal of Applied Glass Science*, vol. 3, no. 2, pp. 89–106, 2012.

[66] K. K. Phani, "Strength distribution and gauge length extrapolations in glass fibre," *Journal of materials science*, vol. 23, pp. 1189–1194, 1988.

[67] P. Zinck, M. Pay, R. Rezakhanlou, and J. Gerard, "Mechanical characterisation of glass fibres as an indirect analysis of the effect of surface treatment," *Journal of Materials Science*, vol. 34, no. 9, pp. 2121–2133, 1999.

[68] B. Bergman, "On the estimation of the weibull modulus," *Journal of Materials Science Letters*, vol. 3, no. 8, pp. 689–692, 1984.

[69] A. G. Clare, P. F. Wachtel, and J. D. Musgraves, "Halide glasses," *Springer Handbook of Glass*, pp. 595–616, 2019.

[70] G. Quinn, “NIST recommended practice guide: fractography of ceramics and glasses, special publication (NIST SP), national institue of standards and technology, gaiterhsburg, md,” 2020.

[71] D. Uhlmann, *Elasticity and Strength in Glasses: Glass: Science and Technology*, vol. 5. Elsevier, 2012.

[72] H. Li, C. Richards, and J. Watson, “High-performance glass fiber development for composite applications,” *International Journal of Applied Glass Science*, vol. 5, no. 1, pp. 65–81, 2014.

[73] L. Yang and J. Thomason, “Effect of silane coupling agent on mechanical performance of glass fibre,” *Journal of Materials Science*, vol. 48, pp. 1947–1954, 2013.

[74] P. Harinath, N. Radadia, S. Bramhe, D. Surendran, V. Sabane, A. Singh, T. N. Kim, R. Sharbidre, B. J. Cheol, L. Peters, *et al.*, “Analysis of microstructural, thermal and mechanical properties of unidirectional glass fiber fabrics exhibiting sizing migration,” *Composites Part B: Engineering*, vol. 164, pp. 570–575, 2019.

[75] F. Hadi and R. Kadhim, “A study of the influence of zinc oxide on acid resistance of natural rubber composites,” *IOP Conference Series: Materials Science and Engineering*, vol. 871, p. 012076, 06 2020.

[76] S. Igheghe, M. Fajobi, and J. Okeniyi, “Anticorrosion behaviour of zinc oxide on aluminum in 2 M of hydrochloric acidic solution,” *IOP Conference Series: Materials Science and Engineering*, vol. 1107, p. 012054, 04 2021.

[77] F. Walsh, G. Ottewill, and D. Barker, “Corrosion and protection of metals: II. types of corrosion and protection methods,” *Transactions of the IMF*, vol. 71, pp. 117–120, 08 1993.

[78] A. Sahai and N. Goswami, “Structural and optical investigations of oxygen defects in zinc oxide nanoparticles,” vol. 1665, 12 2014.

[79] F. Ellyin and R. Maser, "Environmental effects on the mechanical properties of glass-fiber epoxy composite tubular specimens," *Composites Science and Technology*, vol. 64, no. 12, pp. 1863–1874, 2004.

[80] R. Jones and D. Betz, "The kinetics of corrosion of e-glass fibers in hydrochloric acid," *Journal of Materials Science*, vol. 39, pp. 5633–5637, 09 2004.

[81] M. Bayat, H. Yang, and F. Ko, "Effect of iron oxide nanoparticle size on electromagnetic properties of composite nanofibers," *Journal of Composite Materials*, vol. 52, no. 13, pp. 1723–1736, 2018.

[82] A. Gupta, M. Bafna, S. Srivastava, R. Khanna, and Vijay, "Study of electromagnetic shielding effectiveness of metal oxide polymer composite in their bulk and layered forms," *Environmental Science and Pollution Research*, vol. 24, pp. 1–8, 01 2021.

[83] M. Rahman, M. Asadul Hoque, G. Rahman, M. Gafur, R. A. Khan, and M. K. Hossain, "Study on the mechanical, electrical and optical properties of metal-oxide nanoparticles dispersed unsaturated polyester resin nanocomposites," *Results in Physics*, vol. 13, p. 102264, 2019.

[84] I. Haider, I. H. Gul, M. A. Umer, and M. M. Baig, "Silica-fiber-reinforced composites for microelectronic applications: Effects of curing routes," *Materials*, vol. 16, p. 1790, Feb. 2023.

[85] S. Ray, *Silica Fiber-Reinforced Polymer Composites*, vol. 1, pp. 339–362. 03 2012.

[86] K. Iimura, T. Oi, M. Suzuki, and M. Hirota, "Preparation of silica fibers and non-woven cloth by electrospinning," *Advanced Powder Technology - ADVANCED POWDER TECHNOLOGY*, vol. 21, pp. 64–68, 01 2010.

[87] E. Ringdalen and M. Tangstad, "Softening and melting of sio2, an important parameter for reactions with quartz in si production," in *Advances in Molten Slags, Fluxes, and Salts: Proceedings of the 10th International Conference on Molten Slags, Fluxes and Salts 2016* (R. G. Reddy, P. Chaubal,

P. C. Pistorius, and U. Pal, eds.), (Cham), pp. 43–51, Springer International Publishing, 2016.

[88] K. Imoto, M. Sumi, G. Toda, and T. Suganuma, "Optical fiber drawing method with gas flow controlling system," *Journal of Lightwave Technology*, vol. 7, no. 1, pp. 115–121, 1989.